공학석사학위논문

The Effect of Nitrogen and Sulfur Dopants on the Visible Light Photocatalytic Activity of TiO_2

TiO_2의 가시광활성능에 미치는

질소와 황 도펀트의 영향에 대한 연구

2014 년 2 월

서울대학교 대학원

재료공학부

정 준 호

The Effect of Nitrogen and Sulfur Dopants on the Visible Light Photocatalytic Activity of TiO_2

TiO_2의 가시광활성능에 미치는

질소와 황 도펀트의 영향에 대한 연구

지도교수 곽 승 엽

이 논문을 공학석사 학위논문으로 제출함

2014 년 1 월

서울대학교 대학원

재료공학부

정 준 호

정 준 호의 공학석사 학위논문을 인준함

2014 년 1 월

위 원 장 _____ (인)

부위원장 _____ (인)

위 원 _____ (인)

ABSTRACT

The effects of nitrogen and sulfur dopants at inside and surface of TiO_2 was discussed separately to investigate the reasons for the high visible light photocatalytic activity of nitrogen and sulfur codoped TiO_2 (NST). Crystallization and formation of anatase phase of NSTs were observed by X-ray diffraction spectra and high resolution-transmittance electron microscopy (HR-TEM). X-ray photoelectron spectroscopy (XPS) analysis revealed that nitrogen and sulfur atoms are doped at oxygen site of inside of TiO_2 while nitrogen is located in substitutional site and sulfur shows shifted sulfide peak on the surface of TiO_2. The quantity of dopants at oxygen site is significantly decreased with crystallization of NST at high temperature (> 350 °C). As the thermal treatment progressed, sulfur dopants at oxygen site move to surface of NST and finally form sulfate bonding while total amount of sulfur dopants of NST is maintained. UV-Vis diffuse reflectance spectroscopy (DRS) showed that both dopants on the surface and inside of TiO_2 reduce band gap energy. The photocatalytic activities of NST were evaluated by the degradation of rhodamine B (RhB) under visible light and UV light irradiation. Results showed that both of dopants in inside of TiO_2 and surface of TiO_2 enhance visible light photocatalytic activity and act as recombination centers simultaneously. When visible light is irradiated, nitrogen dopants at oxygen site in inside of the TiO_2 enhance solution bulk reaction because they

reduce band gap energy. Sulfide on the surface of NST enhances the surface reaction by interacting with organic dyes. As-synthesized NST has 7.7 times faster degradation rate than that of P25 under visible light irradiation.

Keywords

N, S codoped TiO_2, photocatalyst, photocatalytic activity,

visible light, dopant

***Student number*: 2012-20634**

CONTENTS

1. Introduction

Titanium dioxide (TiO_2) is one of the most widely studied semiconductor for photocatalytic applications such as water splitting, air and water purification, and prevention of stains due to its high photocatalytic activity, low toxicity, high chemical and biological stabilities, and low cost. [1, 2]. The mechanism of photocatalytic reaction is described in figure 1. However, it is hard to use TiO_2 as a photocatalyst under visible light irradiation because of its high band gap energy (3.2 eV for anatase, figure 2). For this reason, great interests have been focused on improving the response of TiO_2 for visible light which comprise 45% of sunlight [3, 4]. Representative methods to enhance visible light response of TiO_2 are described in scheme 1. Introducing other components such as noble metals, organic dyes and semiconductors has been reported. However, these methods have limits for enhancing visible light photocatalytic activity because charge carrier is lost during it is injected to TiO_2. Therefore, doping other elements at TiO_2 has attracted great attention. Band gap narrowing by dopants is depicted in figure 4. These doped TiO_2 can be synthesized easily and show high visible light photocatalytic activity.

In order to reduce the band gap and increase the visible light photocatalytic activity of TiO_2, there have been persistent efforts to incorporate various dopants [5] such as transition metals (Fe, Mo, Ru, Os, Re, V, and Rh) [6-11] and non-metal dopants

(B, C, N, O, F, and S) [12-21]. It is reported that visible light absorbance of TiO_2 can be enhanced by transition metal doping , but only limited amount of transition metal ions should be doped because they act as recombination centers and make conflicting results on the visible light photocatalytic activity of TiO_2 [8-11, 22]. Unlike transition metal dopants, non-metal dopants less likely act as recombination centers, so non-metal doped TiO_2 has been studied intensively [10, 13]. Among various non-metal elements, nitrogen and sulfur receive great attention because they can enhance the visible light photocatalytic activity of TiO_2 efficiently [14, 23, 24]. The number of research papers of non-metal doped TiO_2 is shown in figure 5. It is well known that nitrogen is doped in substitutional oxygen site or interstitial site [13, 15, 16]. Asahi *et al* [17] reported that nitrogen doped in substitutional oxygen site of TiO_2 plays an important role in enhancing visible light photocatalytic activity. On the other hand, other researchers suggest that presence of interstitially doped nitrogen atom makes higher photocatalytic activity under visible light irradiation [18, 19]. Although sulfur is hard to be doped in TiO_2 matrix because of its large ionic radius, sulfur receives great attention as a promising dopant for visible light active TiO_2 [20, 21, 26]. Ohno *et al.* [25] revealed that sulfur atoms move from oxygen site to surface of TiO_2 and form sulfate during crystallization. Many articles show that these sulfate ions on the surface increase the photocatalytic activity of TiO_2 [25, 26]. Recently, further studies reported that N, S

codoped TiO_2 could show higher photocatalytic activity than that of N or S single-doped TiO_2 [14, 23, 24].

Usually, this N and S codoped TiO_2 photocatalysts are simply synthesized by wet chemistry like sol-gel or solvothermal process. To get enough crystallinity for the high photocatalytic activity, most experiments conducted post thermal treatment at high temperature (> 350 °C). Although this post thermal treatment increases the crystallinity and performance of catalysts, it also has negative effects for the photocatalytic activity. Thermal treatment at high temperature cause agglomeration and deterioration of photocatalytic activity [27, 28]. Furthermore, it is also reported that quantity of nitrogen dopant is decreased very significantly when thermal treatment temperature is increased above 400 °C, decreasing photocatalytic activity [15]. Various researches have studied the effect of nitrogen and sulfur doping for the visible light active TiO_2. However, most researches were carried out into the catalysts prepared with post thermal treatment at high temperature. Several groups reported that nitrogen and/or sulfur doped TiO_2 could have high visible light photocatalytic activity without thermal treatment at high temperature which drives the crystallization of TiO_2 [27-31]. Zhao *et al.* studied the effect of thermal treat temperature on photocatalytic activity of nitrogen doped TiO_2. They concluded that nitrogen doped TiO_2 treated at low temperatures (200–250 °C) shows highest visible light photocatalytic activity despite of its high concentration of nitrogen and low crystallinity. This result implies

that surface functional groups or nitrogen inside of TiO_2 could be an important factor for visible light activity. Changseok *et al.* [26] reported that after the thermal treatment at 350 °C for 2 h, sulfur doped TiO_2 film showed higher photocatalytic activity than that of other samples which is treated at high temperature (450 and 500 °C). These results showed that it is possible to use nitrogen and/or sulfur doped TiO_2 as a visible light active photocatalyst without post thermal treatment at high temperature.

However, most researches have not discussed the role of nitrogen and sulfur codopants in detail. Especially, dopants exist both inside and surface of TiO_2 before the crystallization, but there are no studies that consider the effect of dopants on the surface and inside of N, S codoped TiO_2 separately. For these reasons, detail study on the effect of nitrogen and sulfur dopants for the photocatalytic activity of TiO_2 without thermal treatment at high temperature is needed.

In present study, we investigate the effect of nitrogen and sulfur dopants for the photocatalytic activity of TiO_2. Nitrogen and sulfur codoped TiO_2 (NST) was simply synthesized by solvothermal method and post thermal treatment at various temperatures (200–400 °C) was applied. Chemical states and quantity of nitrogen and sulfur dopants at surface and inside of NSTs were observed separately by XPS spectra. These results were considered with the results of characteristics and photocatalytic activity of NSTs to identify the effect of dopants. This study could provide the understanding of the effect of nitrogen and sulfur dopants for the high visible light

photocatalytic activity of TiO_2 and suggest efficient way to prepare the highly visible light active TiO_2.

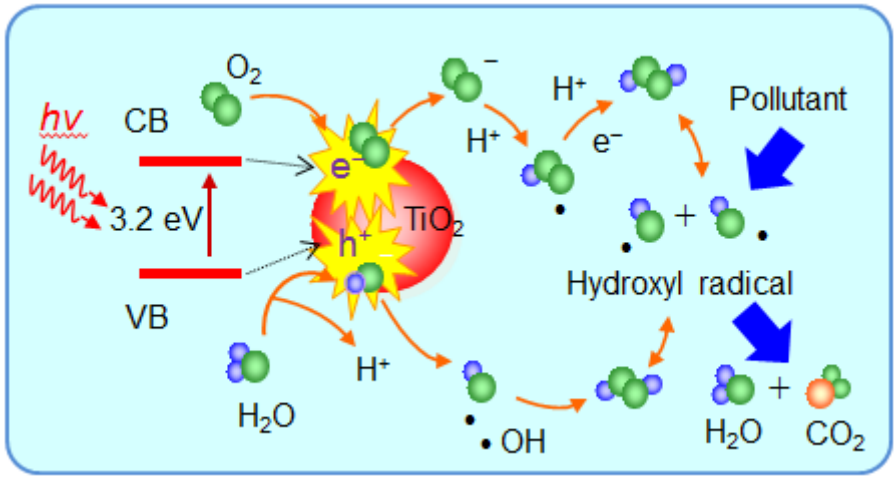

Figure 1. Mechanism of photocatalysis of TiO_2 in water

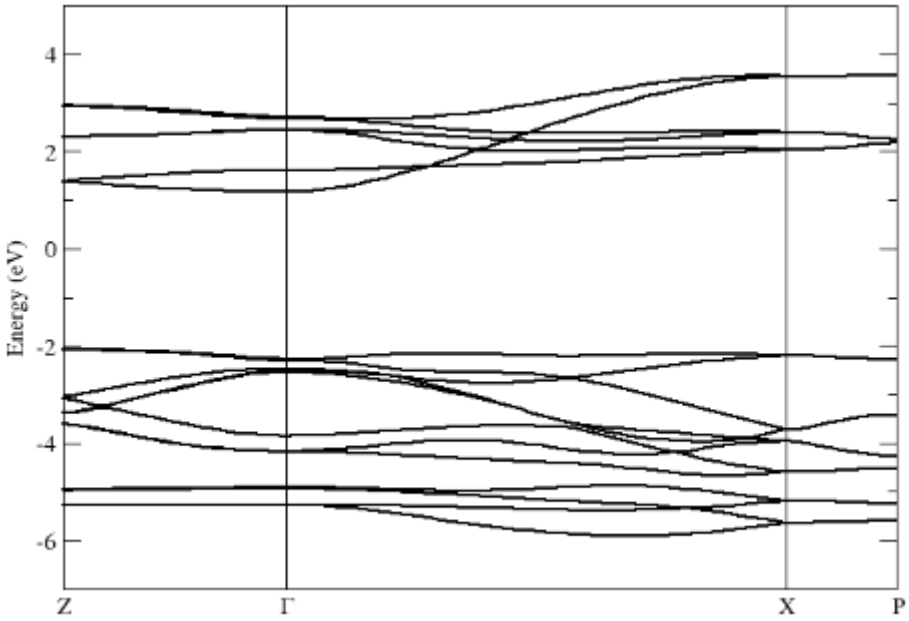

Figure 2. Calculated band structure of anatase TiO_2

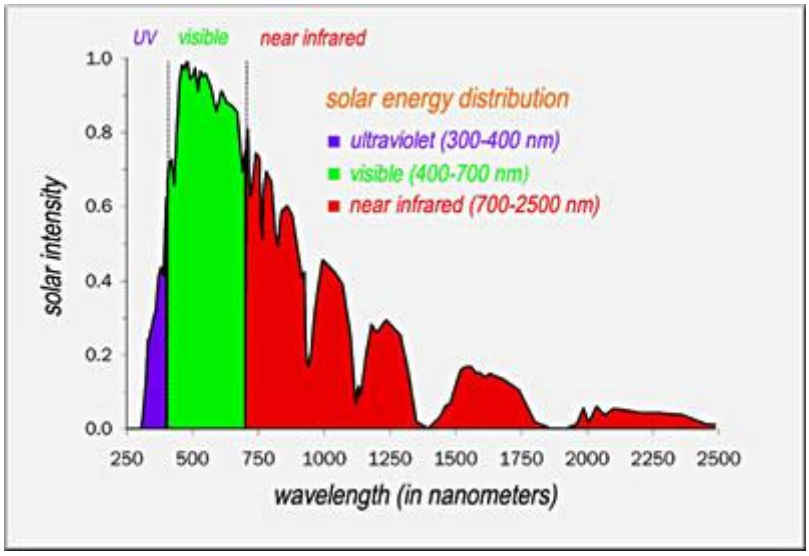

Figure 3. The spectrum of sunlight

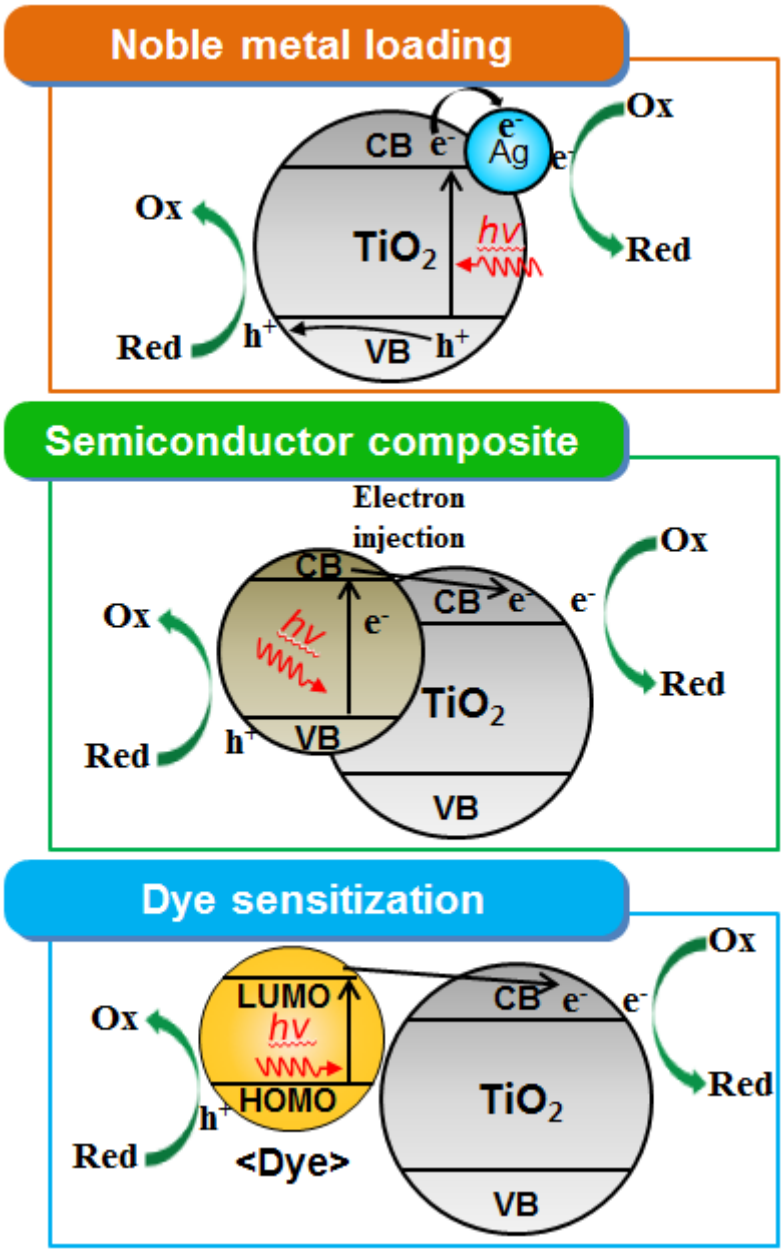

Scheme 1. Schematic description of visible light active TiO_2

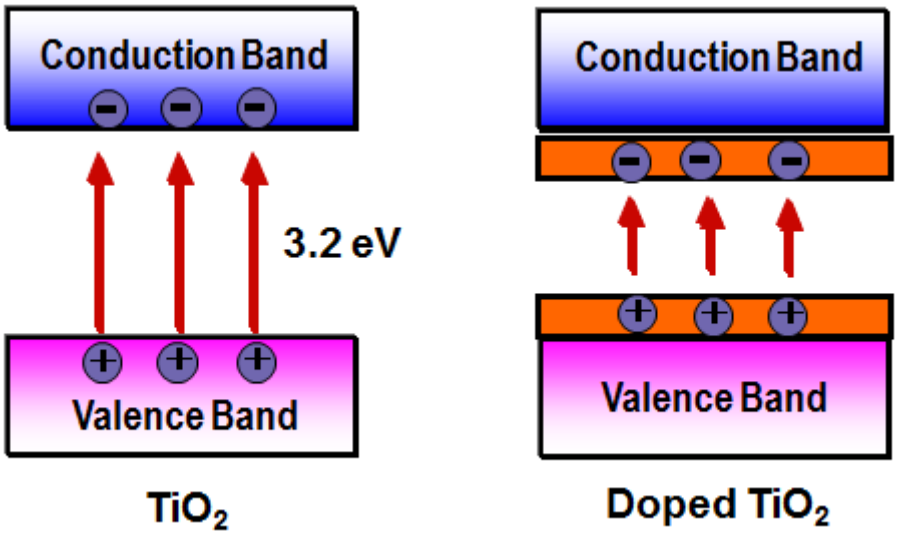

Figure 4. Band gap narrowing by dopants

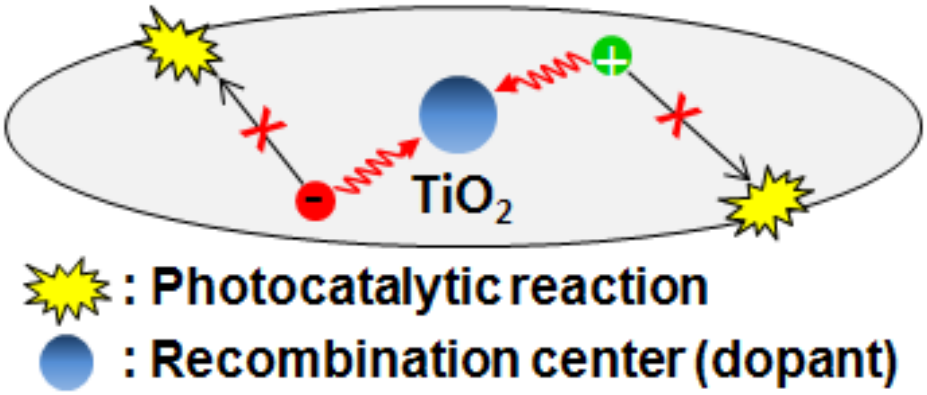

Scheme 2. Recombination of charge carriers by dopant

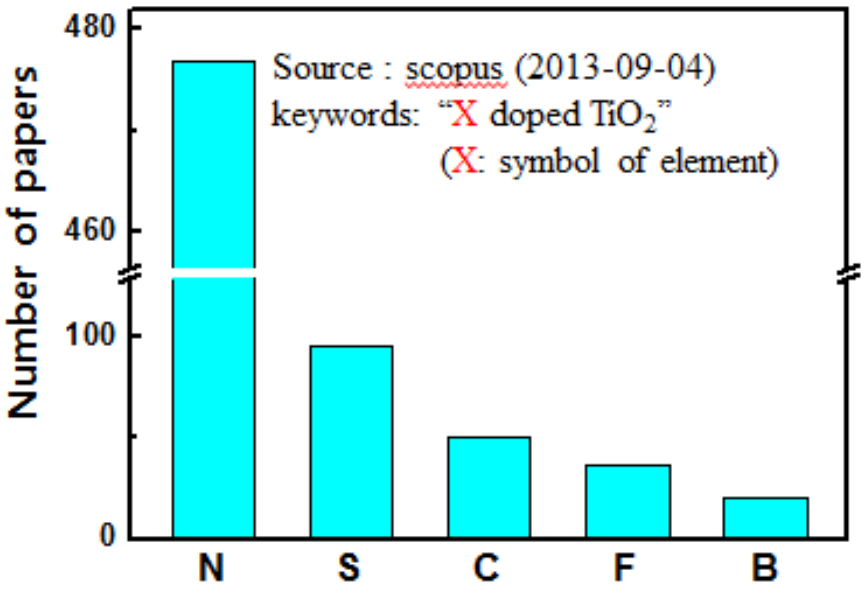

Figure 5. Number of papers of non-metal doped TiO2

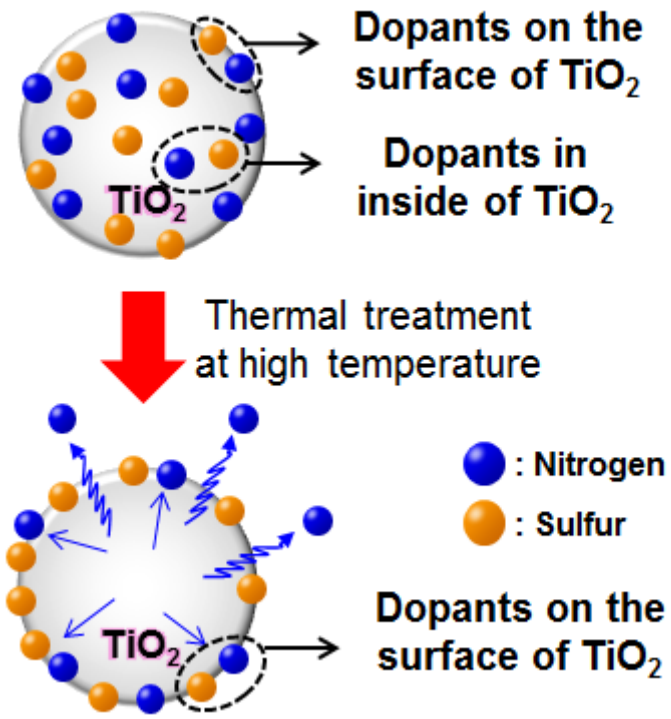

Scheme 3. Thermal behaviors of nitrogen and sulfur dopants

2. Experimental

2.1. Materials

Titanium (IV) isopropoxide (TTIP, $Ti(OPri)_4$), 2,4-pentanedione (AcAc, $C_5H_8O_2$), thiourea, and absolute ethanol were all purchased from Sigma-Aldrich and used as received without further purification. Highly deionized water with resistivity of 18.0 MΩ cm−1 was used throughout the experiments.

2.2. Preparation of N, S codoped TiO_2

N, S codoped TiO_2 were prepared on 2 steps. First, N, S codoped TiO_2 with enough crystallinity and dopants contents was synthesized by solvothermal treatment. After that, as-synthesized sample is treated at various temperatures. To identify the effect of crystallization, thermal treatment is conducted from low temperature (200 °C) to high temperature (400 °C)which makes crystallization of TiO_2.

2.2.1 Step 1: Synthesis of nitrogen and sulfur codoped TiO_2 (NST-As) by solvothermal treatment

Thiourea was used as a dopant source. 0.02 mol of thiourea was dissolved sufficiently in 70 mL of absolute ethanol to get solution A. 0.02 mol of TTIP and 0.04 mol of AcAc were dissolved in 30 mL of absolute ethanol to get solution B. Then solution B was added to solution A under vigorous stirring. After the mixing of two solutions, 2 mL of deionized water was added to the solution. After stirring for 10 minutes, the solution was transferred to a 170 mL Teflon-lined stainless-steel autoclave and heated at 115 °C for 12 hours. After the solvothermal treatment, the autoclave was cooled down at room temperature. The resulting yellow powder was collected and washed several times with deionized water and methanol by centrifugation. It is dried in vacuum oven at 50 °C for 24 hours.

2.2.2 Step 2: Post thermal treatment process

As-synthesized nitrogen and sulfur codoped TiO_2 (NST) was thermally treated at 200, 250, 300, 350, 400 °C. Quantity of as-synthesized sample was 0.2 g in one ceramic pot. First, temperature of furnace is elevated from room temperature to thermal treatment temperature. The rate of temperature increase was 5 °C min−1. When the temperature reaches to thermal treatment temperature, temperature of furnace is maintained for 2 hours. After the thermal treatment, samples were cooled down

slowly in air. These NSTs are named as NST-As (as-synthesized sample) or NST-x (x: thermal treatment temperature).

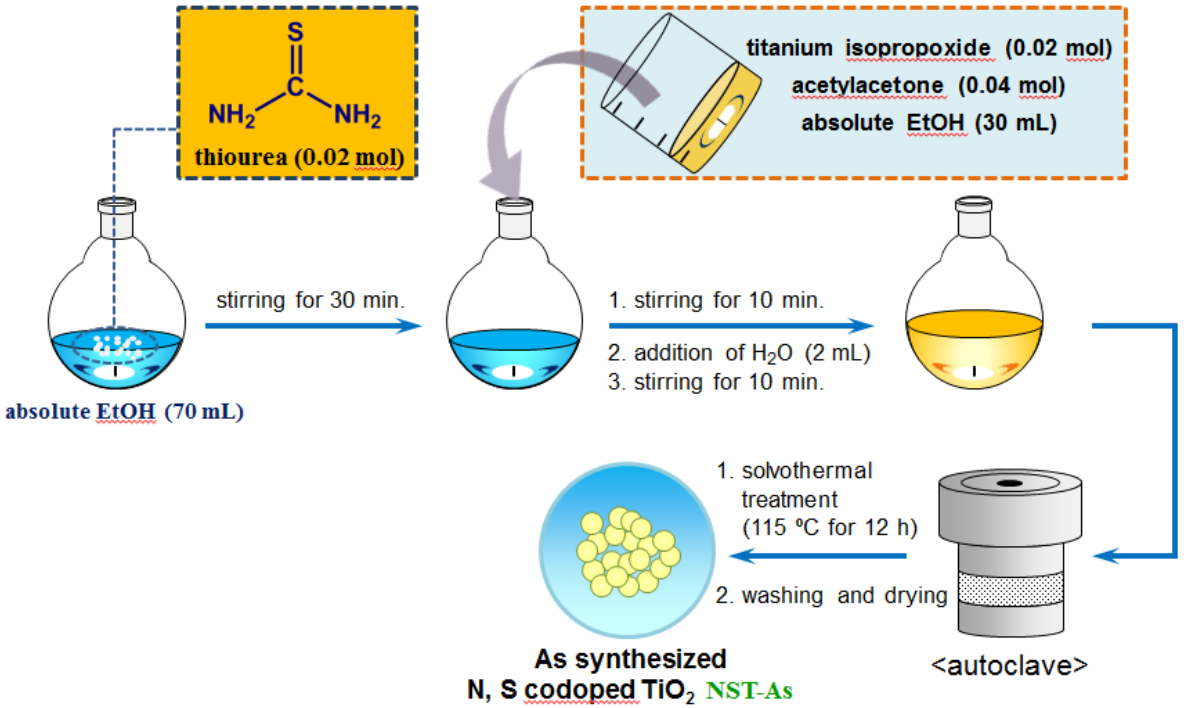

Figure 6. The synthesis of NST-As

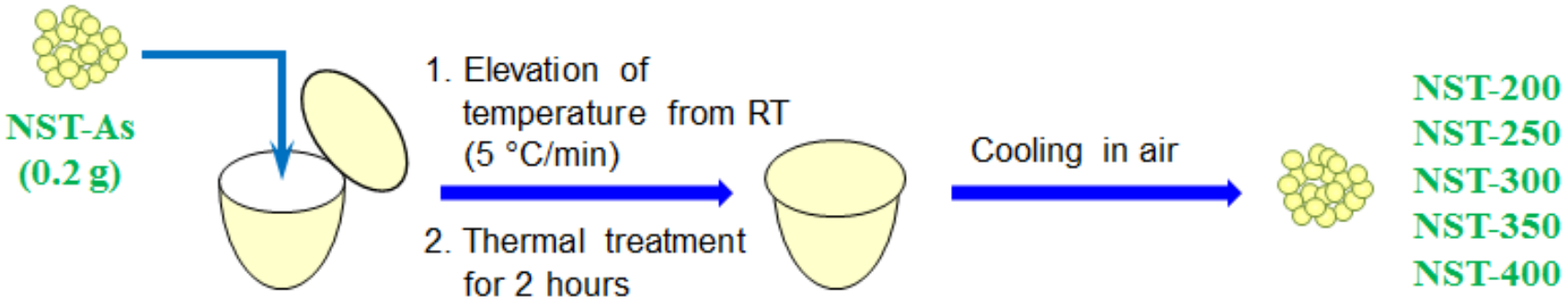

Figure 7. Post thermal treatment of NST-As

2.3. Characterization of synthesized NSTs

2.3.1. Crystal structure, crystal size and surface area

The crystal structures and crystal sizes were investigated by X-Ray diffraction (XRD, New D8 Advance) in a 2θ range of 20–80° by using Cu Kα radiation as a X-ray source (λ = 0.154 nm). The crystallite sizes were obtained by using the Scherrer equation ($\Phi = K\lambda/\beta\cos\theta$), where Φ is the crystallite size, λ is the wavelength of the X-ray irradiation, K is usually assumed taken as 0.89, β is the full width at half-maximum intensity (FWHM), and θ is the diffraction angle of the (101) peak for anatase TiO_2. The morphologies and crystal structures were observed by high resolution transmission electron microscopy (HR-TEM, JEM-3010). The specific surface areas were calculated by the Brunauer-Emmett-Teller (BET) equation, and pore size distributions were determined by the Barrett-Joyner-Halenda (BJH) formula.

2.3.2. Quantity and chemical state of dopants

The chemical states and quantities of dopants were characterized by X-ray photoelectron spectroscopy (XPS, AXIS-Hsi) by using monochromatic Mg Kα radiation as X-ray source. All of the binding energies were calibrated to the C1s peak at 284.5 eV. XPS TiO_2 analysis was done for not only dopants on the surface of TiO_2 but also dopants inside of TiO_2. To observe the chemical states and quantities of dopants inside of NSTs, argon etching was performed by argon ion for 10 minutes with a sputtering rate of 0.3 nm min-1. The relation between the thermal treatment temperature and atomic ratio of sulfur to titanium was determined by inductively coupled plasma atomic emission spectroscopy (ICP-AES, Optima 4300DV) with argon plasma source at 6,000 K.

2.3.3. Thermal behaviors

Thermal behaviors of NST-As were observed by thermogravimetric analysis (TGA). Analysis was carried out in the temperature range of 25–700 °C and the rate of temperature increase was 5 °C/min.

2.3.3. Band gap energy measurement

Absorbance of NSTs at visible light region was observed by UV-Vis diffuse reflectance spectroscopy (UV-DRS, Cary 5000). The surface areas and pore size distributions of the NSTs were characterized by nitrogen adsorption-desorption isotherm measurement.

2.4. Photocatalytic activity and adsorptivity evaluation

The photocatalytic activity of NSTs was evaluated by measuring the degradation of RhB in an aqueous solution. Evaluation was carried out under visible light and ultraviolet light irradiation. The adsorptivity of NSTs was evaluated in MB solution.

2.4.1. Rhodamine B degradation test under visible light irradiation

Before the evaluation, NSTs were dispersed by sonication for 30 minutes. To remove residual organic by-product, UV light was irradiated to NSTs solution. These procedures are depicted in scheme 4. The visible light photochemical reactor was made up of one commercial 400 W halogen spotlight and quartz glass beaker. The reactor is shown in figure 8 (a). The solution inside of beaker was composed of 150 mL of deionized water, 60 mg of NSTs, and 15 mg of RhB. The temperature of reactor was maintained at 36 ±1 °C by four air coolers and distance between lamp and beaker was 200 mm.

2.4.2. Rhodamine B degradation test under UV light irradiation

Before the evaluation, same process as above sonication and UV irradiation is conducted. The reactor for evaluation of UV light photocatalytic activity was made up of four lamps producing 15 W UV-A and quartz glass beaker. The solution for the photocatalytic reaction was composed of 150 mL of deionized water, 15 mg of catalyst, and 15 mg of RhB. The temperature of reactor was 50 °C and distance between each lamps and beaker was 120 mm. UV light photochemical reactor is drawn in figure 8 (b).

2.4.3. Adsorption test in rhodamine B and methylene blue solution

Adsorptivity of catalyst for RhB was evaluated under the same condition as visible light photochemical reactor condition, with beaker wrapped by aluminium foils. The concentration of RhB was obtained by UV-Vis spectrometer (Lambda 25) in range 400–700 nm. A commercial TiO_2, P25 was selected as a reference photocatalyst and evaluation was performed under the same experimental conditions. Methylene blue (MB) adsorption and degradation test was carried out in the same condition as RhB degradation test under visible light irradiation for 4 hours.

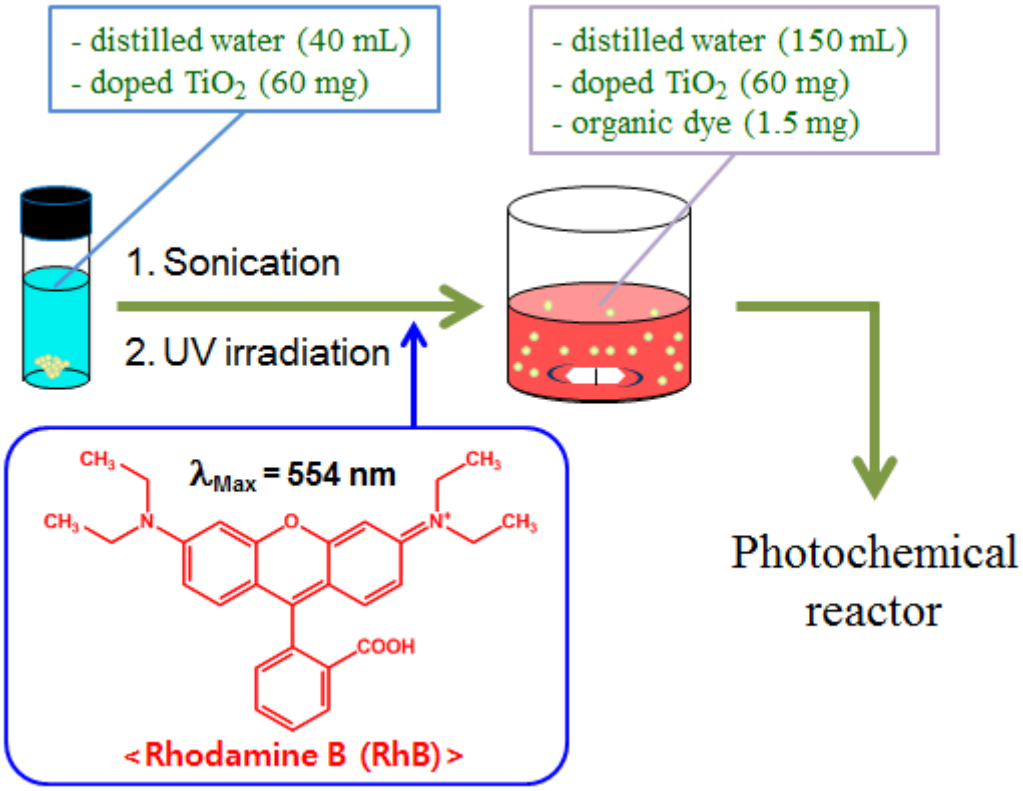

Scheme 4. The procedure of photocatalytic activity evaluation

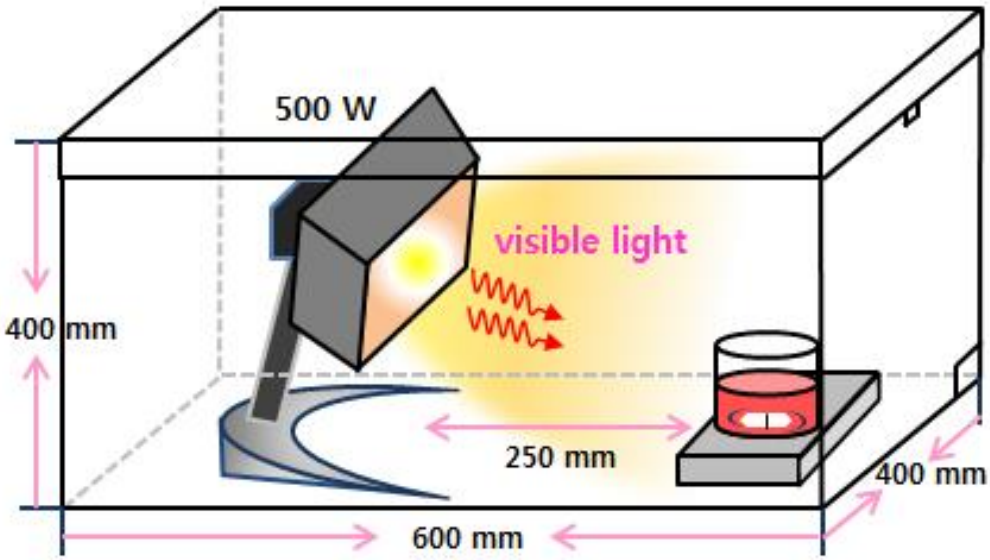

Figure 8 (a). The visible light photochemical reactor

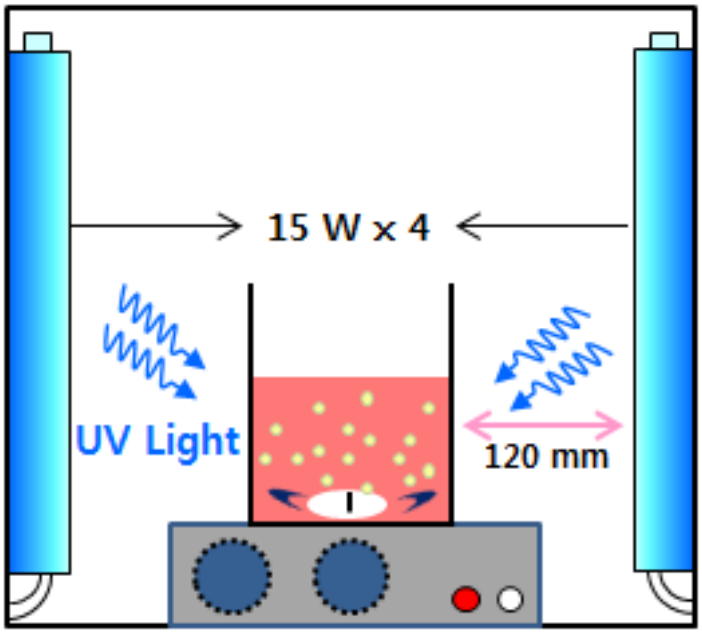

Figure 8 (b). The UV light photochemical reactor

Table 1. Photocatalytic activity evaluation conditions

Light source	Visible light	UV light
Temperature	36 ± 1 °C	50 ± 1 °C
Distance from light source	250 mm	120 mm
Interval/evaluation time	2 h / 10 h	10 min / 40 min

3. Results and Discussion

3.1 Characterization of synthesized NSTs

3.1.1. Crystal structure and crystal size and surface area

Figure 9 shows the XRD patterns of all NST samples. All samples have anatase TiO_2 crystal structure, without rutile or brookite phases. It is found that NST-As has weak and broad anatase TiO_2 (101) and (200) peaks. These broad peaks could be attributed to low crystallinity or small size of crystals [31]. When thermal treatment temperature is lower than 350 °C, there are no remarkable changes of XRD patterns of NSTs. The intensity of anatase peak is increased when thermal treatment temperature is higher than 350 °C. Crystal sizes obtained by Scherrer equation from anatase peak (101) are shown in table 2. Crystal sizes of NST-As and NST-200, 250, 300 have similar crystal sizes around 4 nm. Crystal sizes of NST-350 and NST-400 are increased rapidly with crystallization of TiO_2.

Figure 10 shows the HR-TEM images and FFT analysis of NSTs. It is found that NST-As is composed of agglomerated small nano-sized crystals. It implies that the shape of XRD pattern of NST-As is come from not only low crystallinity but also small size of nano crystal. FFT fame shows that crystals have anatase structure and (101) plane is dominant. TEM images of NST-350 and NST-400 show more clear crystal structure and higher crystal size because of crystallization of TiO_2.

Specific surface areas of NSTs and P25 are written in table 3. All of NSTs have relatively higher surface areas than that of P25 because of their small crystal sizes. It is known that interface nucleation dominates the transformation of TiO_2 at low temperature [28]. There are mild decreases of surface area from NST-200 to NST-300 because transformation rate is slow and interface nucleation is dominant at low temperature. NST-350 and NST-400 have relatively low surface area because transformation rate is fast at high temperature so small crystals merge into larger crystals. These results can be confirmed by observation of pore size distribution in figure 11. NST-As, 200 and 250 have similar pore size distribution while NST-300, 350 and 400 have more large pores because of mass transfer. It is well matched with the results of XRD patterns.

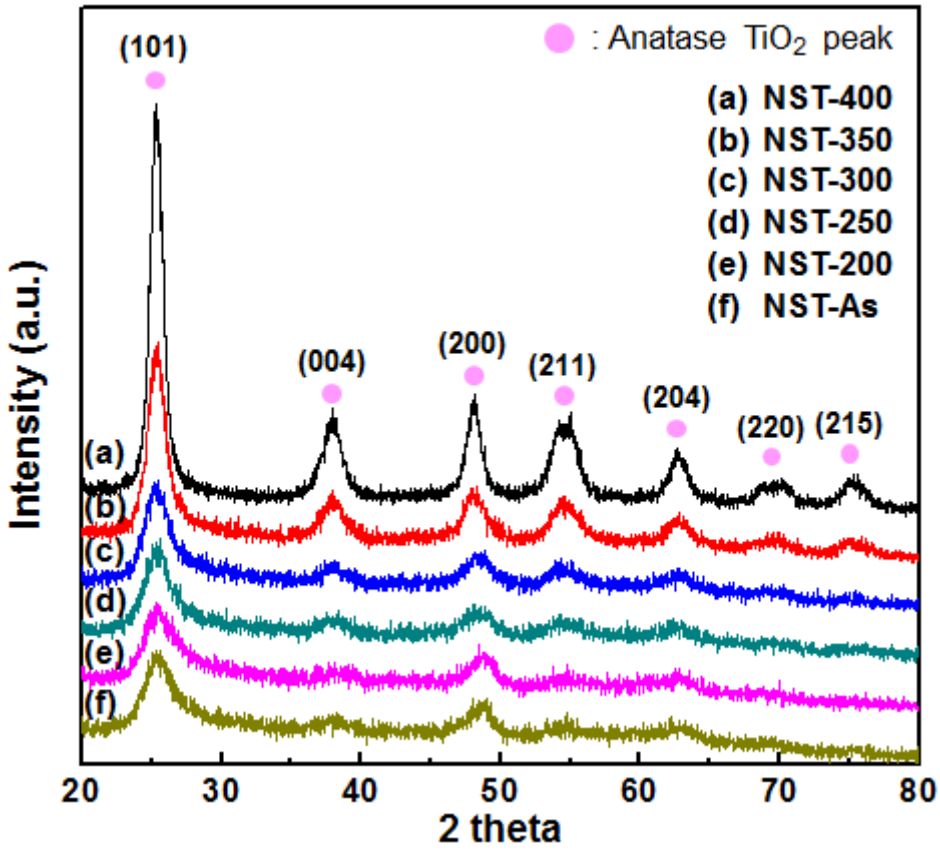

Figure 9. XRD patterns of NSTs treated at different temperatures

Table 2. Crystal sizes of NSTs obtained by Scherrer equation

Sample	Crystal size (nm)
NST-As	4.21
NST-200	3.85
NST-250	4.77
NST-300	4.62
NST-350	6.54
NST-400	8.45

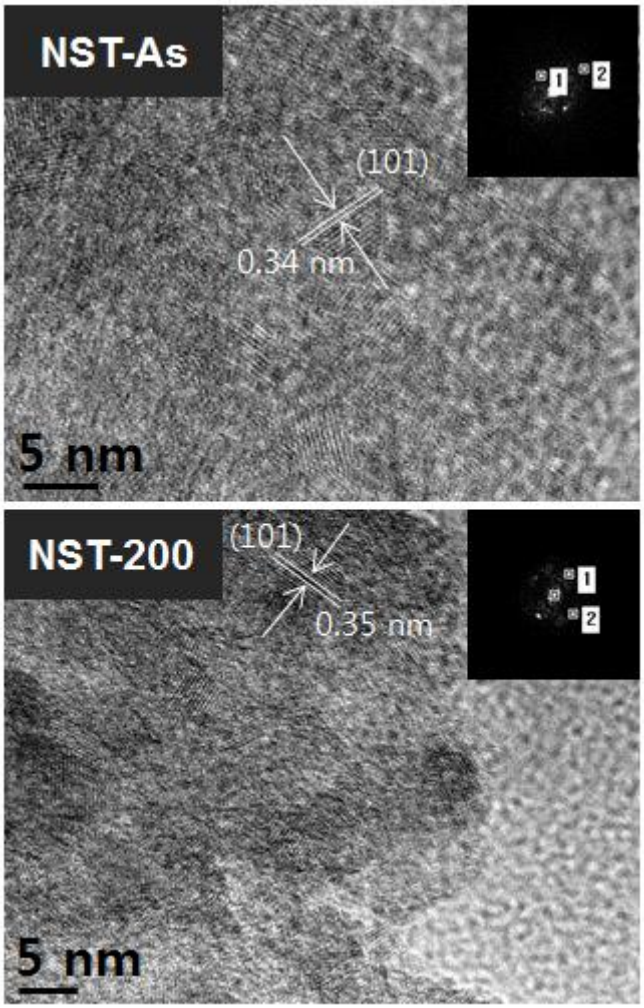

Figure 10 (a). HR-TEM images of NST-As and 200

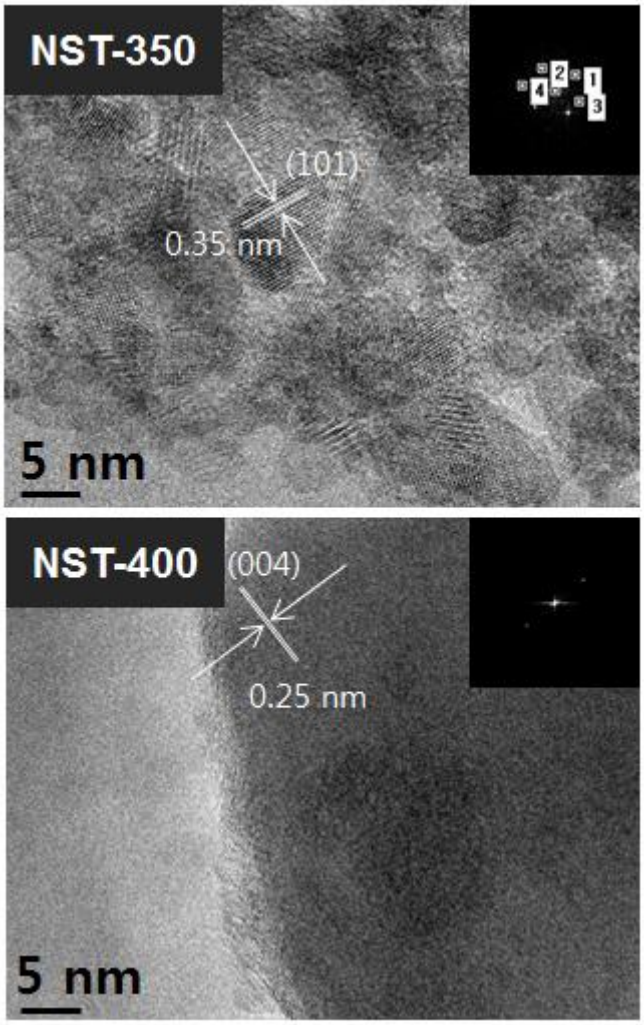

Figure 10 (b). HR-TEM images of NST-350 and 400

Table 3. brunauer-Emmett-Teller (BET) surface area of NSTs and P25

Sample	Surface area (m_2/g)
P25	51.4
NST-As	291.5
NST-200	253.9
NST-250	242.3
NST-300	232.7
NST-350	207.2
NST-400	121.3

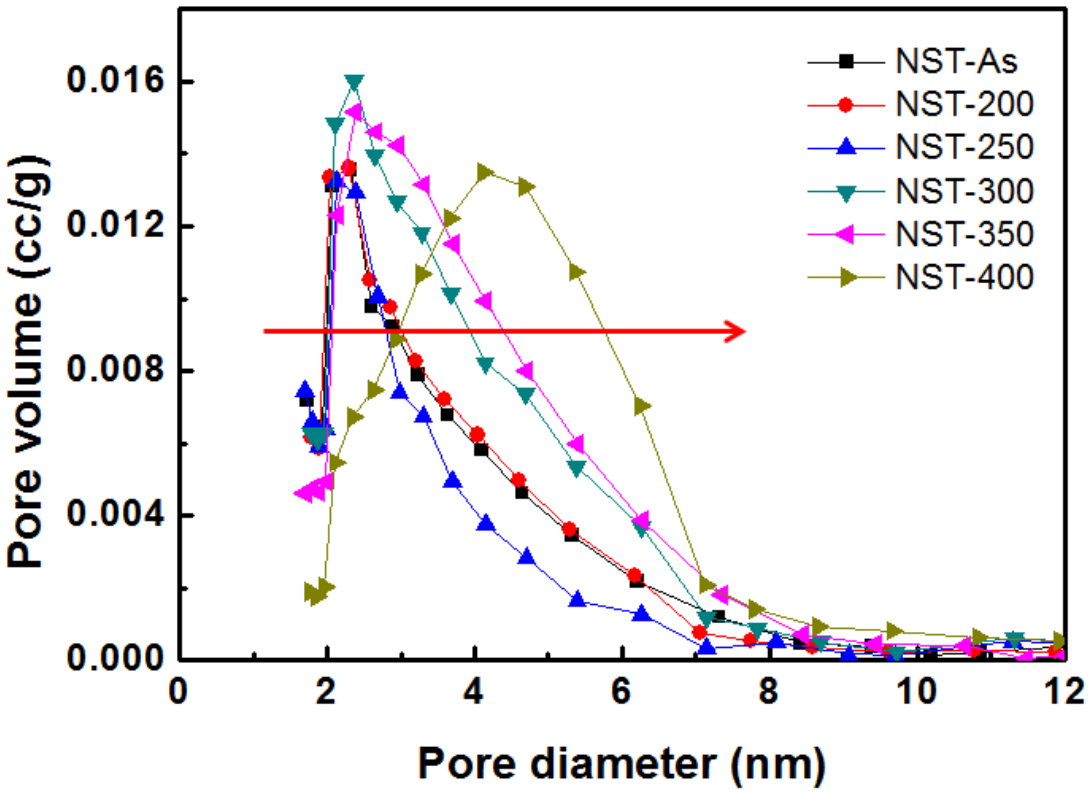

Figure 11. Pore size distribution of NSTs obtained by Barrett-Joyner-Halenda method

3.1.2. Quantity and chemical state of dopants

Chemical states and quantities of dopants are shown in figure 12. Dopants at surface and inside of NSTs are treated respectively. In figure 12 (a), all N 1s peaks have higher binding energy than 400 eV, which means nitrogen on the surface of TiO_2 is located in interstitial site and bonded with titanium and oxygen atoms regardless of thermal treatment. However, another peak at lower binding energy region is observed after Ar^+ etching in figure 12 (b). This peak is contributed to the fact that nitrogen dopants are located in oxygen site and bonded with titanium atoms. It can be found out that quantity of nitrogen dopants located in inner oxygen site and interstitial site of TiO_2 is rapidly decreased with the crystallization of TiO_2. These results suggest that nitrogen is doped at oxygen site during solvothermal process while nitrogen dopants on the surface of TiO_2 are combined with oxygen atoms and have high binding energy for 1s electrons.

It is found that sulfur on the surface of NST-As shows shifted peak around 164 eV. This peak is neither sulfide ($S2^-$) nor sulfate ($S6^+$) peaks which were reported in most research for the sulfur doped TiO_2. After the Ar^+ etching, sulfur dopants which substitute oxygen atoms are detected. The quantity of sulfur dopants on the surface of NST-As is similar to that of sulfur dopants at oxygen site of NST-As. And ICP-AES results show that the quantities of sulfur are constant regardless of thermal treatment temperature (table 4). Therefore, the shifted peak on the surface of NST-As can be

considered as a peak for sulfur dopants doped on the surface of TiO_2, not for organic by-product. Sulfur dopants which substitute oxygen atoms in the lattice of TiO_2 is bonded with three titanium atoms which have relatively low electronegativity. Because of neighbor titanium atoms which have low electronegativity, electrons in sulfur 2p orbital have relatively low binding energy. In case of sulfur on the surface of NST-As, it is considered that sulfur dopants more likely make bonds with other atoms such as hydrogen or oxygen which have higher electronegativity than that of titanium because sulfur has large ionic radius and it makes the insertion of sulfur into the TiO_2 lattice more difficult [20, 32]. This shifted peak cannot be found in other samples, which means that the sulfur on the surface of NST-As is reactive and easily deformed by thermal treatment even though the temperature is low (~200 °C). Sulfate is formed on the surface of TiO_2 when thermal treatment temperature is higher than 300 °C. Like the nitrogen dopants, concentration of sulfur dopants at oxygen site is decreased rapidly with crystallization of TiO_2.

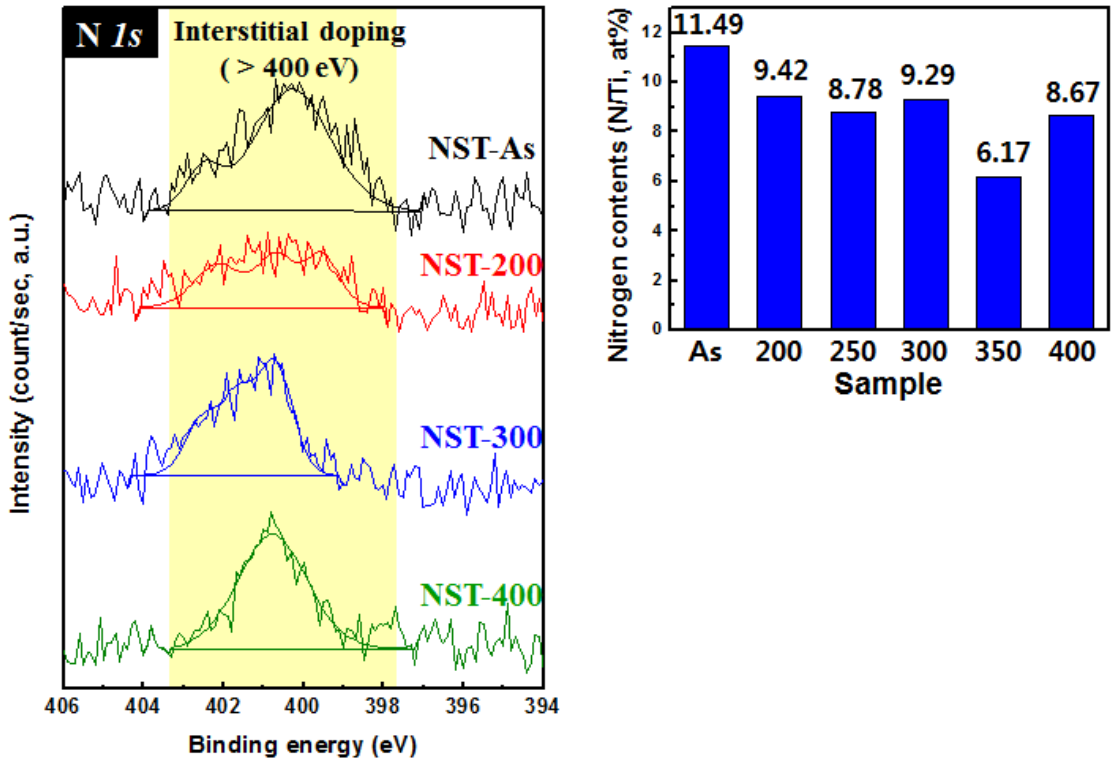

Figure 12 (a). Quantity and chemical state of nitrogen dopants on the surface of NSTs

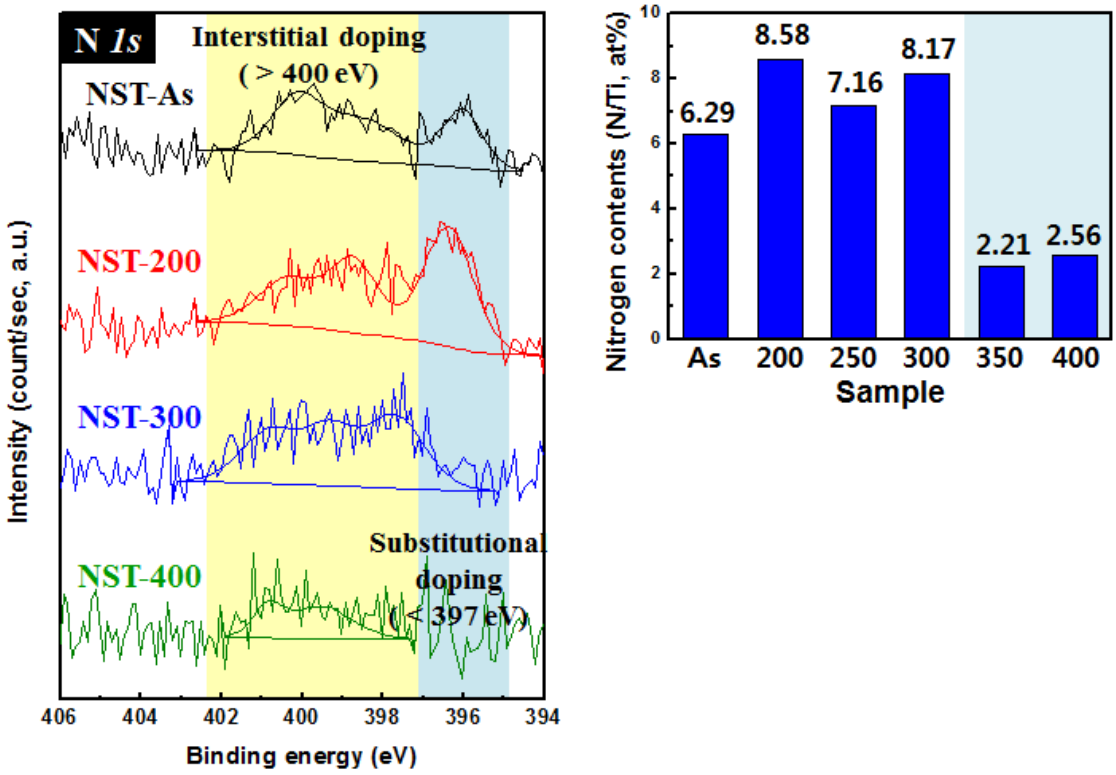

Figure 12 (b). Quantity and chemical state of sulfur dopants at inside of NSTs

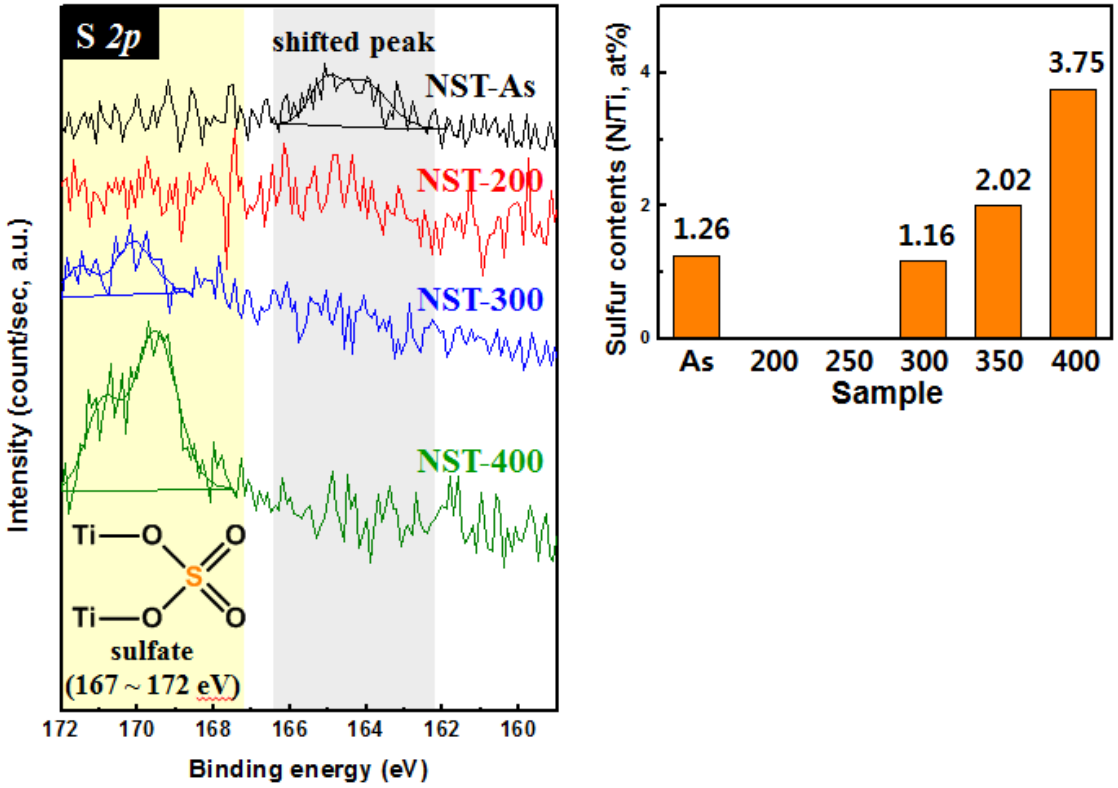

Figure 12 (c). Quantity and chemical state of sulfur dopants on the surface of NSTs

Table 4. Relative concentrations of sulfur dopants in NSTs measured by ICP-AES

Sample	NST-As	NST-200	NST-250	NST-300	NST-350	NST-400
S/Ti (at%)	0.99	1.00	0.97	1.06	1.05	1.07

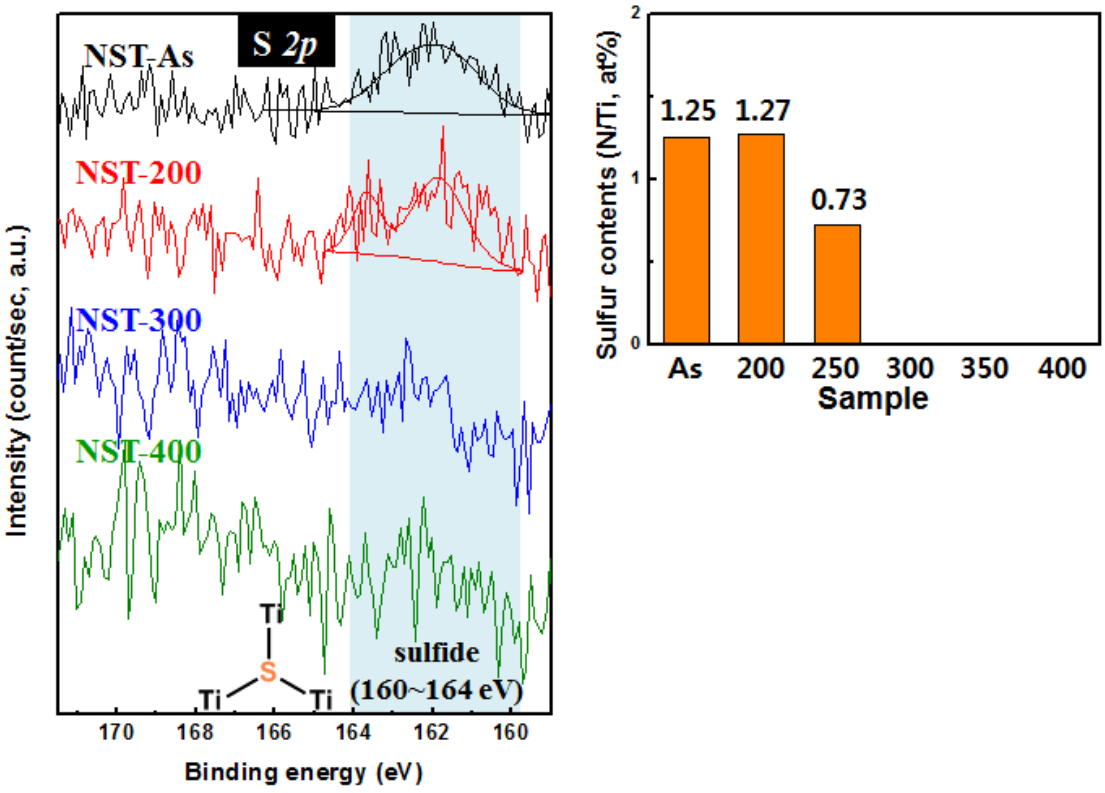

Figure 12 (d). Quantity and chemical state of sulfur dopants at inside of NSTs

3.1.3. Thermal behavior

Thermal behaviors of NST-As is depicted in figure 13. Adsorbed water or solvent were removed at low temperature (< 100 °C). Around 200 °C, weight of NST-As is decreased rapidly because organic by-products are degraded. When the temperature is higher than 300 °C, crystallization is progressed and dopants at inside of TiO_2 are removed. Figure 13 shows that weight of NST-As is decreased when dopants are removed from TiO_2 with crystallization. When the temperature is higher than 500 °C, NST-As shows no change of weight.

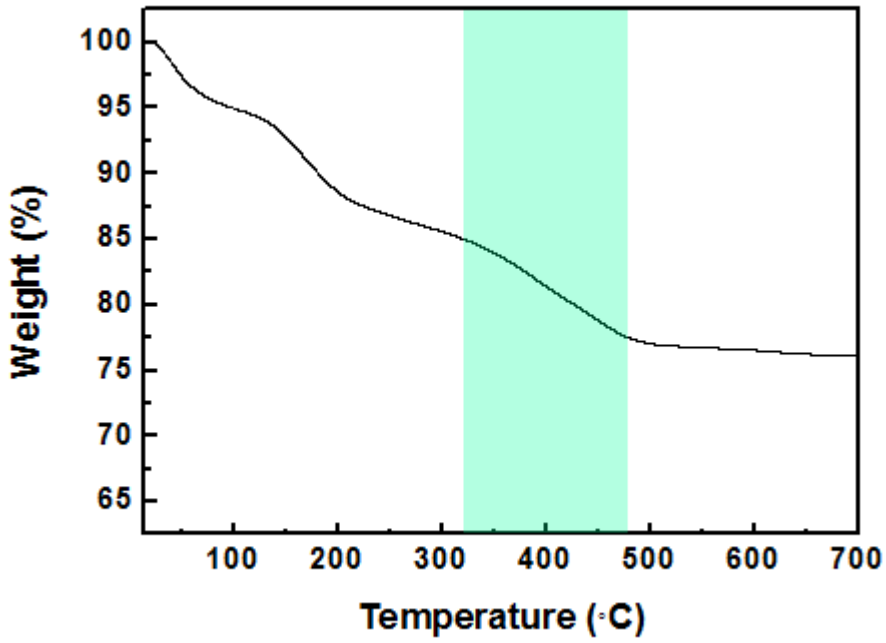

Figure 13. Thermogravimetric analysis of NST-As

3.1.4. Band gap energy

Absorbance at visible light region of NSTs and P25 is shown in figure 5. NST-As, 200, 250 and 300 have high absorbance at visible light region while NST-350 and NST-400 show less red shift. Band gap energy was obtained by Kubelka-Munk equation

$$F(R) = \frac{(1-R)^2}{2R} \quad \text{(Eq. 1)}$$

where R is reflectance. Band gap energies of NSTs are shown in table 5. NST-As has band gap energy of 2.85 eV which is lower than that of pure TiO_2 (3.30 eV). Band gap energy of NST-350 and NST-400 (3.21 eV) are slightly smaller than that of P25. NST-350 and NST-400 have lower band gap energy than P25 because of existence of dopants on the surface of NST-350 and 400. These results demonstrate that both of dopants on the surface and inside of TiO_2 reduce band gap energy. Ho *et. al.* [30] reported that response of TiO_2 for visible light increases with the quantity of sulfur dopants doped at oxygen site. However, absorbance of sulfur doped TiO_2 is relatively smaller than that of NST-As although quantities of sulfur at oxygen site of sulfur doped TiO_2 (> 1.5 at%) are higher than that of NST-As (1.26 at%). It suggests that nitrogen dopants at oxygen site in TiO_2 play an important role in band gap narrowing of NST-As compare to small amount of sulfur dopants at oxygen site of NST-As. These results are well matched with the loss of nitrogen dopants described in figure 4 (b), because it

was known that nitrogen make narrow band gap when nitrogen and sulfur are codoped in TiO_2 [24]. When nitrogen substitutes oxygen, nitrogen dopant forms delocalized state slightly above the valence band of TiO_2 [33]. Irie et al. [34] reported that nitrogen doped TiO_2 has low quantum efficiency under visible light irradiation when concentration of nitrogen dopants which substitute oxygen atoms is lower than 1 at% because nitrogen atoms at oxygen site make an isolated narrow intra band, instead of making narrow band gap. On the other hand, it was shown by calculation that mixed N 2p and O 2p states make narrow band gap when nitrogen substitutes 6 at% of oxygen in TiO_2 [17]. Figure 4 (b) and figure 5 show that high contents of nitrogen doped at oxygen site make highly visible light active TiO_2 because it makes wide intra band.

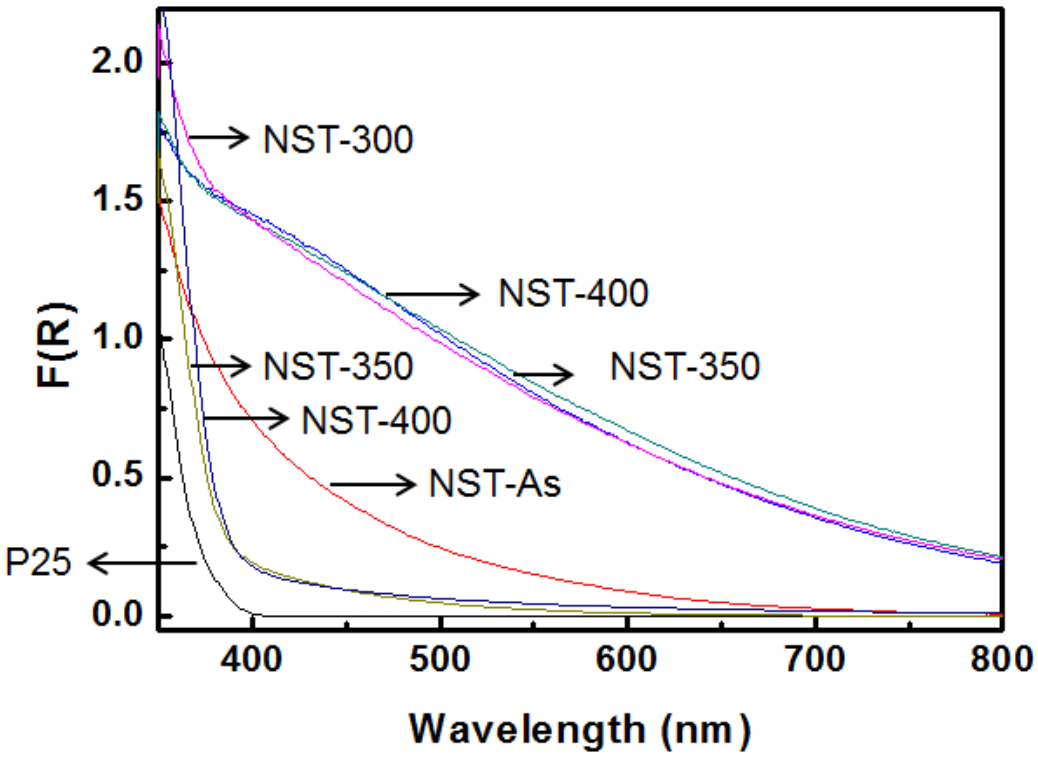

Figure 14. Thermogravimetric analysis of NST-As

Table 5. Band gap energies of NSTs and P25

Sample	P25	NST-As	NST-350	NST-400
E_g (eV)	3.30	2.85	3.21	3.21

3.2. Photocatalytic activity and

3.2.1. Mechanisms of degradation of rhodamine B by pure TiO_2

To analysis the effect of dopants, mechanisms of degradation of rhodamine B should be identified. It is reported that pure TiO_2 has two different pathways for the degradation of organic dyes under visible light and UV light irradiation [35]. These two mechanisms are illustrated in figure 15. When visible light is irradiated, pure TiO_2 cannot generate electron-hole pair because it has a wide band gap. However, organic dyes such as RhB respond to visible light and induce electrons. When organic dyes adsorb on the surface of TiO_2, these electrons are injected to the conduction band of TiO_2 and generate hydroxyl radical. This hydroxyl radical interacts with RhB which is adsorbed to TiO_2 and induces de-ethylation of RhB. Therefore, exchange of charge carriers between TiO_2 and organic dyes by surface reaction determines the degradation rate when visible light is irradiated to TiO_2. On the contrary, TiO_2 can induce electron by using UV light. These induced electrons make hydroxyl radicals, and hydroxyl radicals are involved in the solution bulk reaction for the direct degradation of organic dyes. Because the solution bulk reaction is usually 3 orders faster than surface reaction, solution bulk reaction is a dominant pathway for degradation of organic dyes under UV light irradiation.

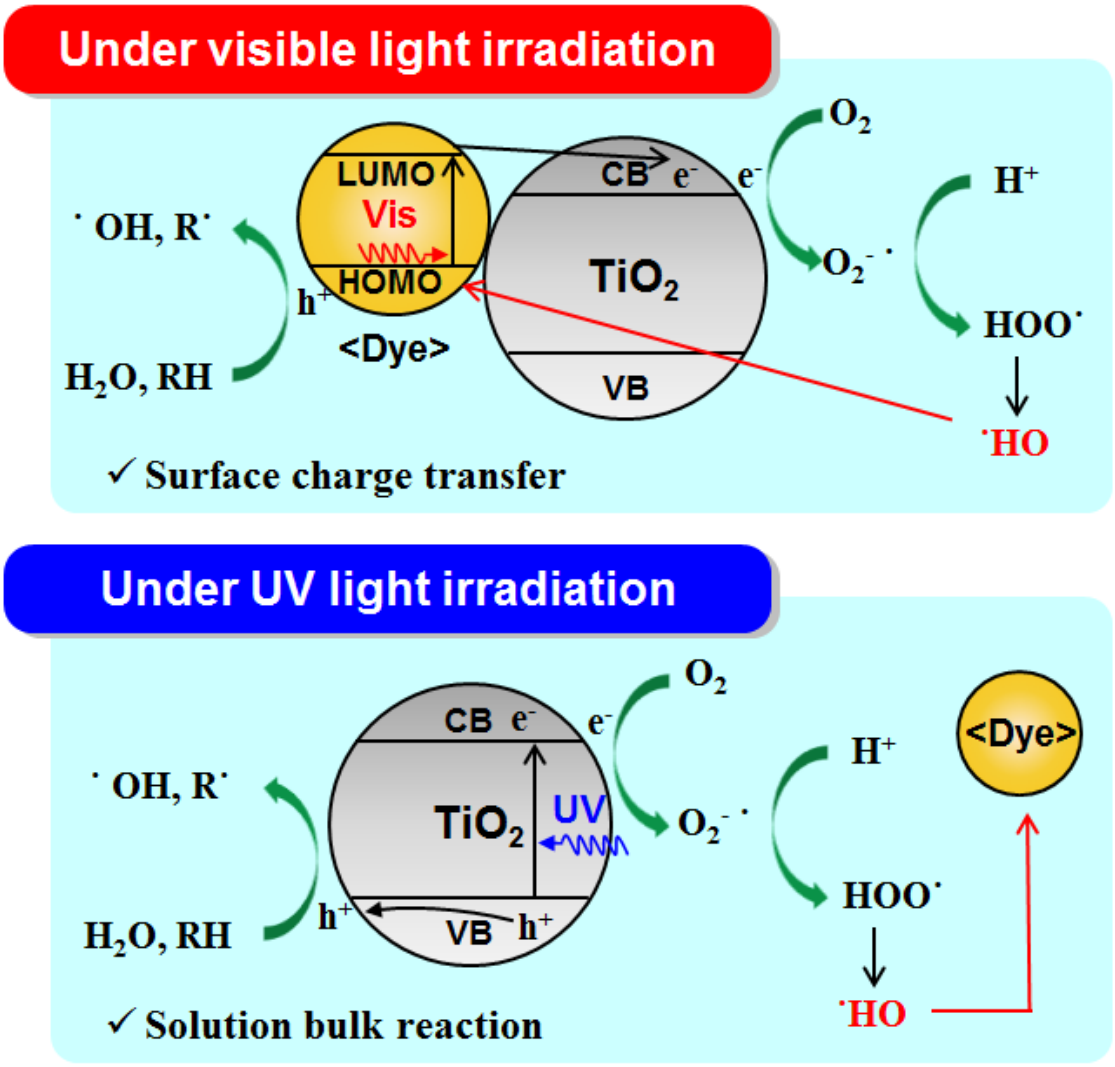

Figure 15. Mechanism of degradation of rhodamine B by pure TiO_2

3.2.2. Visible light photocatalytic activity of NSTs

Figure 18 shows the visible light photocatalytic activities of NSTs and P25. Degradation rate was calculated by the pseudo-first-order equation

$$K_a t = \ln(\frac{C_0}{C}) \quad \text{(Eq 2.)}$$

where K_a is rate constant, t is reaction time, C_0 is initial concentration of RhB and C is interval concentration of RhB. Amount of RhB adsorbed on the surface of NSTs and P25 was less than 13% of initial concentration of RhB (figure 16) and self-degradation rate of RhB without catalyst was negligible compare to the initial concentration of RhB. Results show that NST-As, 200, 250 and 300 have higher visible light photocatalytic activity than that of P25. On the other hand, NST-350 and 400 have relatively low activity compare to P25. This means TiO_2 has high visible light photocatalytic activity when nitrogen and sulfur dopants replace oxygen inside of TiO_2 because it makes red shift by modification of band gap although they act as recombination centers. Especially, NST-As exhibits the highest performance compares to NST-200, 250, and 300. The rate constant of NST-As was 0.901 h^{-1}, which is 7.7 times faster than that of P25 (0.117 h^{-1}). Through the fact that NST-As has higher photocatalytic activity than NST-200, 250 and 300, it can be known that sulfur dopants on the surface of NST-As also enhance the activity. It will be discussed later on. Low photocatalytic activity of

NST-350 and 400 results from the excess amount of dopants on the surface of TiO_2. It has been reported in many researches that nitrogen or sulfur doped TiO_2 which were thermally treated at high temperature have optimized surface dopant concentration because dopants act as recombination centers. In this research, however, concentration of dopant on the surface of TiO_2 was not a targeted variable. For this reason, NST-350 and 400 show low photocatalytic activity compare to P25 even though they have high specific surface area and crystallinity.

The high visible light photocatalytic activities of NSTs can be explained by considering two degradation mechanisms written above. The shape change of UV-Vis spectra of RhB solution under visible light irradiation is described in figure 19. Results reveal that NST-As, 200, 250 and 300 cause rapid de-ethylation. Most of RhB was de-ethylated within 2 hours by NST-As, and NST-200, 250 and 300 de-ethylate RhB in 8 hours while de-ethylation of RhB is not finished after 10 hours. These results confirm that NST-As, 200, 250 and 300 has strong interaction with RhB, so de-ethylation of RhB by surface reaction is enhanced. Furthermore, NST-As shows faster surface reaction rate than that of NST-200, 250 and 300. There are no big differences between NST-As and NST-200, 250 and 300 except the shifted sulfur peak on the surface of NST-As. These results demonstrate that sulfur on the surface of NST-As can interact with RhB and enhance surface reaction.

After the de-ethylation by NSTs, intensity of de-ethylated dye is decreased rapidly. NST-As, 200, 250 and 300 are respond to visible light because they have narrow band gap. Therefore, electrons in the valence band can be excited to the conduction band and participate in the solution bulk reaction unlike the pure TiO_2. Because of increase of solution bulk reaction, NST-As, 200, 250, 300 have relatively high visible light photocatalytic activity.

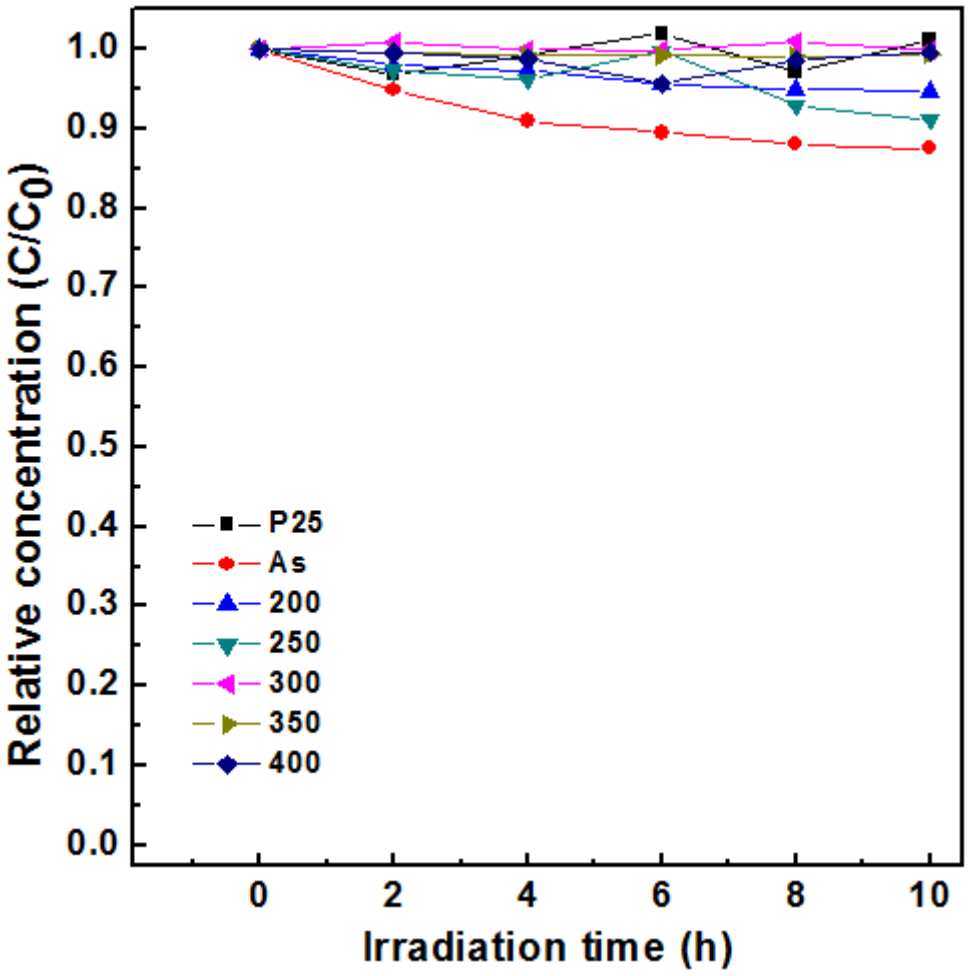

Figure 16. Measurement of adsorptivity of NSTs for RhB

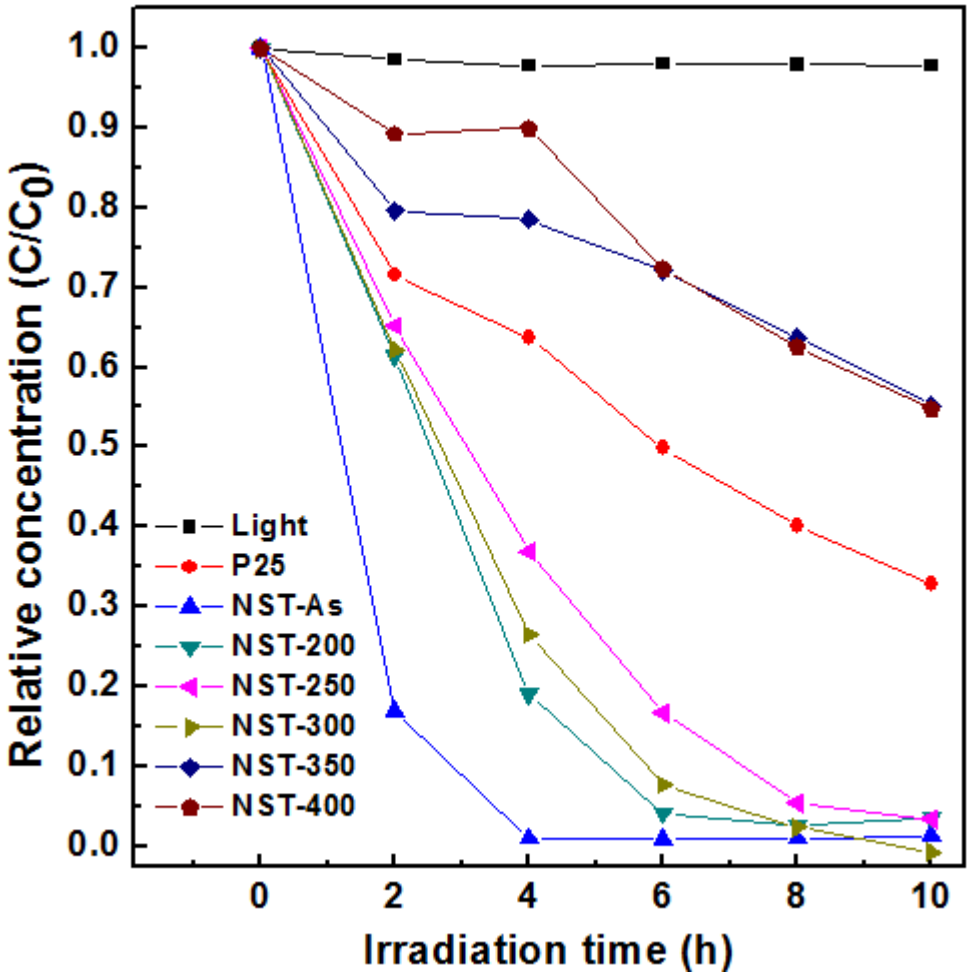

Figure 17. Relative concentration of RhB under visible light irradiation

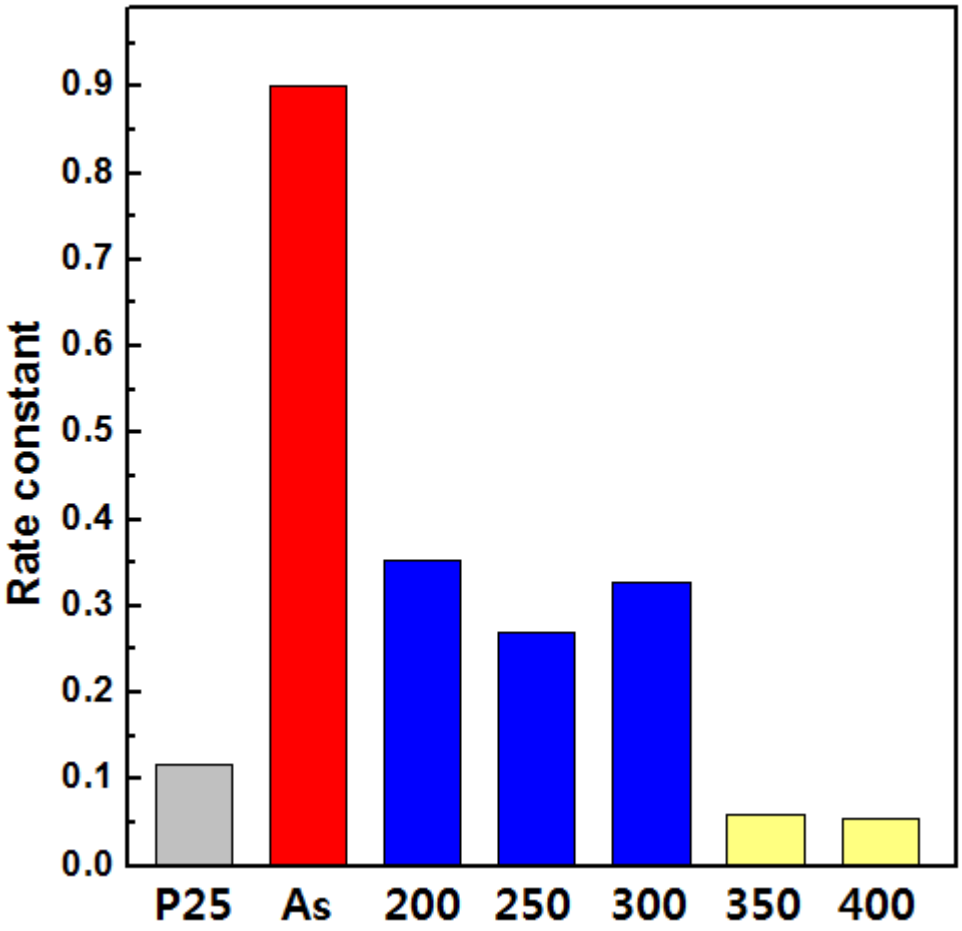

Figure 18. Degradation rate of NSTs and P25 under visible light irradiation

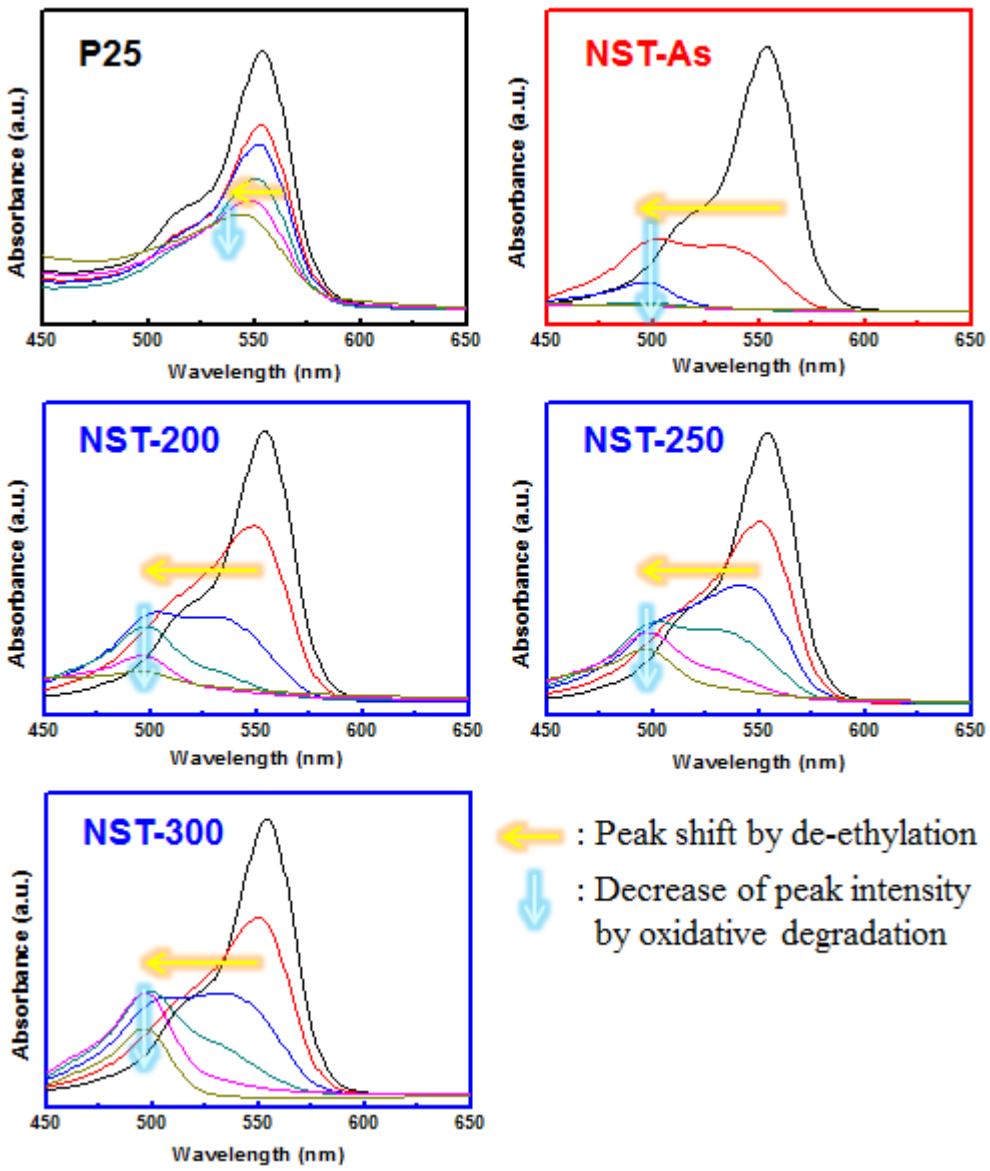

Figure 19. Time-dependent UV-Vis curve of RhB solution obtained by visible light photocatalytic activity test

3.2.3. UV light photocatalytic activity of NSTs

It is revealed in figure 21 that all samples have much low degradation rates compare to P25 under UV irradiation. Degradation rate is gradually decreased when thermal treatment temperature is increased until temperature reaches to 300 °C. When temperature is higher than 300 °C, degradation rate is increased with increase of thermal treat temperature. In the case of UV light irradiation, photocatalytic activity of NST-As, 200, 250 and 300 is significantly decreased compare to visible light photocatalytic activity of them because effect of band gap narrowing by dopants at inside of TiO_2 is diminished while dopants still act as recombination centers. When heat is applied at 350 °C and 400 °C, dopants located in inside of TiO_2 move out from TiO_2 and crystallinity is increased. However, NST-350 and 400 have lower photocatalytic activity compare to P25 than that of NST-350 and 400 under visible light irradiation because dopants on the surface of TiO_2 also deteriorate the photocatalytic activity. These results show that both of dopants in inside of TiO_2 and surface of TiO_2 enhance visible light photocatalytic activity and act as recombination centers simultaneously.

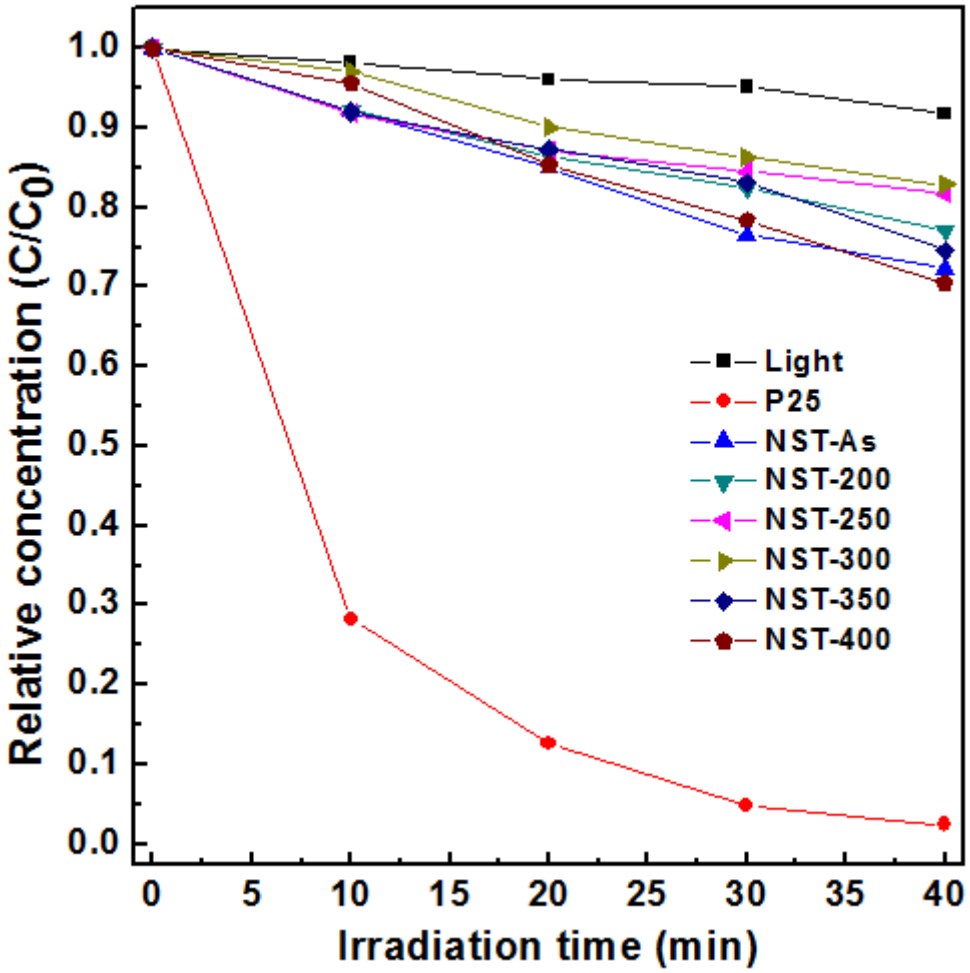

Figure 21. Relative concentration of RhB under UV light irradiation

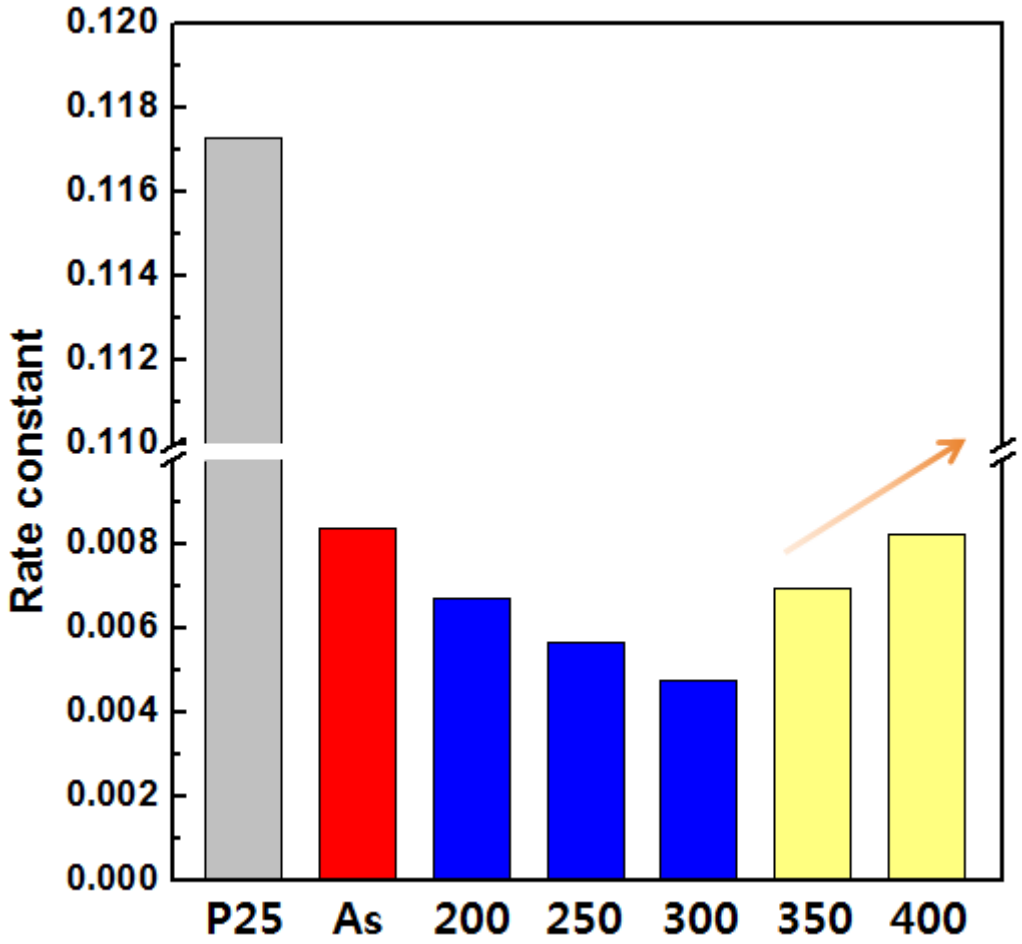

Figure 22. Degradation rate of NSTs and P25 UV light irradiation

3.2.4. Adsorptivity of NSTs in methylene blue solution

In the above discussion, we deduced that sulfur on the surface of NST-As enhances the surface reaction. However, in the case of the adsorption between TiO_2 and RhB, rate of adsorption, surface reaction and desorption are very fast, so it was hard to quantify the difference of surface reaction rate of NSTs. Furthermore, it couldn't be defined clearly what kind of structure sulfur forms. Therefore, we introduce methylene blue adsorptivity evaluation to find out the effect of sulfur more clearly.

It is well known that methylene blue (MB) can be adsorbed to surface of sulfur modified electrode [36]. MB has similar molecular structure as RhB and doesn't have different function groups except one sulfur cation. For these reasons, MB was selected to investigate the effect of sulfur on the surface of NST-As. Ratio of adsorbed MB is shown in table 6. Although initial amount of MB is same as RhB, NSTs adsorb MB much more than RhB. It implies sulfur atom in MB interacts with NSTs. And it can be found that adsorptivity of NSTs is decreased when thermal treatment temperature is increased. When temperature is increased, sulfur on the surface of TiO_2 is changed to sulfate and lose their adsorptivity. It is reported that photocatalytic degradation of MB by TiO_2 starts from the interaction between sulfur cation of MB and oxide anion on the surface of TiO_2 [37]. Therefore, if sulfur dopants substitute oxygen and form sulfide anion on the surface of TiO_2, they should have strong interactions with MB because interaction between two sulfur atoms is strong. High adsorptivity for MB and high

photocatalytic activity for RhB confirm the existence of sulfide anion on the surface of TiO_2. These results indicate that before sulfur dopant is changed to sulfate form by thermal treatment, it should form sulfide anion in deionized water to interact with sulfur cation in MB. The shifted sulfur peak in figure 12 (c) is well matched with this phenomena. Change of quantities of sulfur dopants on the surface of NST-As is described in figure 23. Quantity of sulfur is doubled when MB is adsorbed to NST-As. This is an indirect experimental evidence of the fact that sulfur on the surface of TiO_2 interacts with sulfur in methylene blue. When MB adsorbed NST-As is irradiated by visible light, it is shown in figure 23 (c) that quantity of sulfur is decreased. This result means adsorbed methylene blue on the surface of NST-As is degraded by photocatalytic reaction.

Table 6. Relative amount of MB adsorbed to NSTs and P25

Sample	P25	NST-As	NST-200	NST-250	NST-300	NST-350	NST-400
C/C_0	0	0.86	0.62	0.48	0.37	0	0

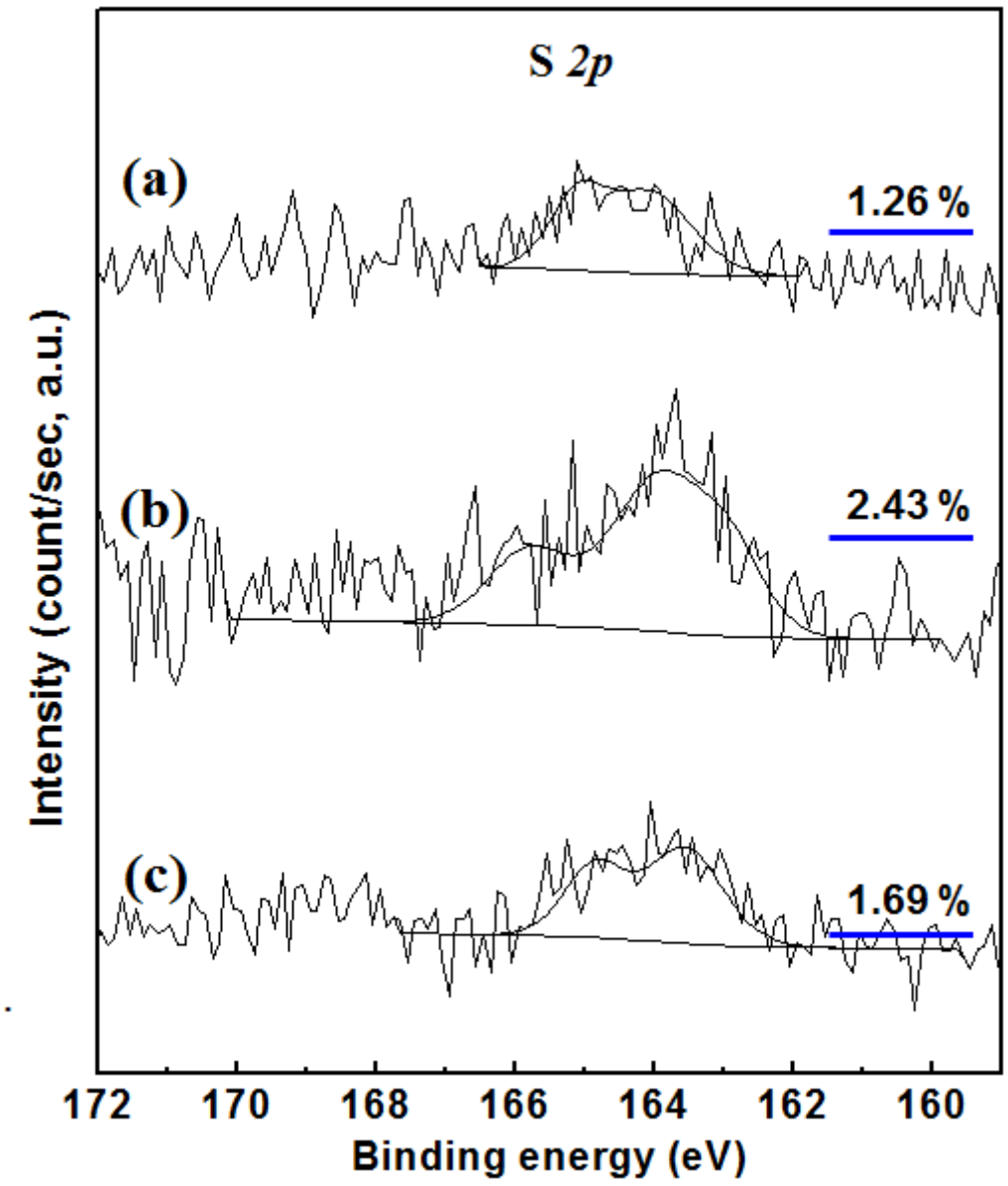

Figure 23. XPS spectra of sulfur on the surface of (a) NST-As, (b) Methylene blue adsorbed NST-As and (c) visible light irradiated NST-As.

3.2.5. Mechanisms of degradation of rhodamine B by NSTs

Effects of nitrogen and sulfur dopants for the visible light photocatalytic activity of TiO_2 are summarized in scheme 5. As written above, sulfide anion on the surface of TiO_2 enhances surface reaction with cation of organic dyes and nitrogen which substitutes oxygen inside of TiO_2 enhances solution bulk reaction under visible light irradiation. However, when UV light is irradiated, solution bulk reaction rates of NSTs are much smaller than that of P25 because dopants act as recombination centers, without positive effect. Furthermore, influence of enhanced surface reaction on the surface of NST-As is negligible compare to P25 because solution bulk reaction is dominant when UV light is irradiated. Therefore, NSTs show much less photocatalytic activity under UV light irradiation. Solution bulk reaction of NSTs was also enhanced because of band gap narrowing by nitrogen dopants at oxygen sites which form delocalized states in the band gap of TiO_2.

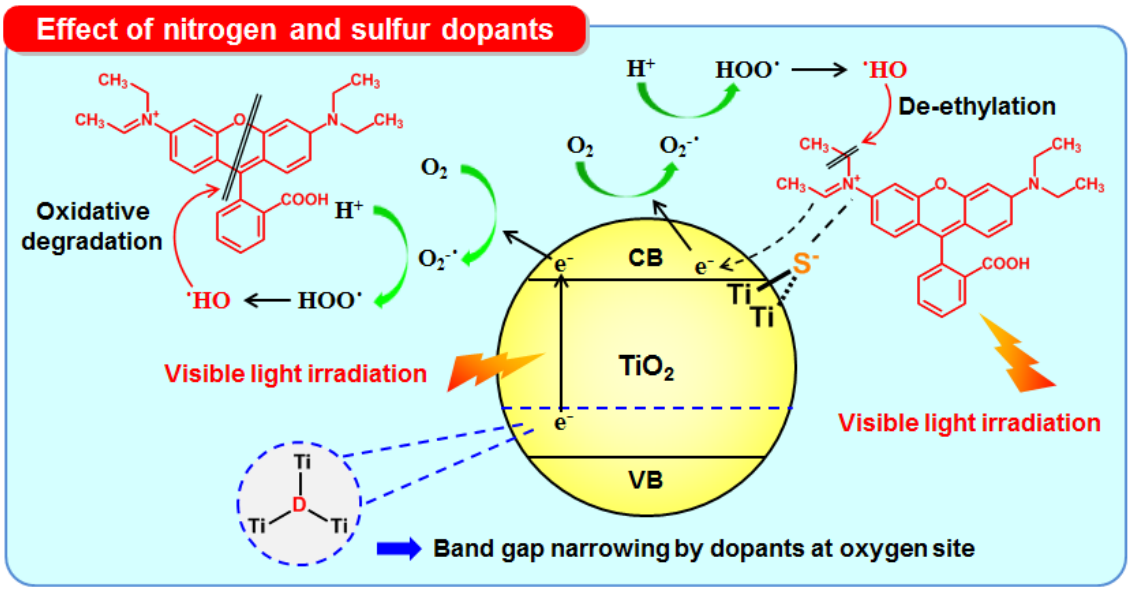

Scheme 5. Effects of visible light photocatalytic activity of NSTs

4. Conclusions

To identify the effect of nitrogen and sulfur dopants for the photocatalytic activity of TiO_2, a series of nitrogen and sulfur codoped TiO_2 were prepared by solvothermal treatment and their photocatalytic activity was evaluated in photocatalytic degradation of rhodamine B under visible light and UV light irradiation. As-synthesized sample is composed of agglomerated nano-sized anatase crystals. XPS results showed that quantities of dopants which substitute oxygen in TiO_2 are rapidly decreased during the crystallization of TiO_2. Nitrogen dopants which substitute oxygen in TiO_2 enhance absorbance at visible light region while dopants on the surface of TiO_2 make only small amount of red shift. It was found that nitrogen dopants at oxygen in TiO_2 enhance visible light photocatalytic activity although they act as recombination centers. When sulfur is doped at oxygen site on the surface of as-synthesized TiO_2, it cannot be bonded with two titanium atoms and its 2p electron has higher binding energy because sulfur has larger ionic radius than that of oxygen. This sulfur promotes surface reaction with organic dyes and makes higher visible light photocatalytic activity. Methylene blue adsorption test confirmed that adsorptivity of samples are decreased with the increasing temperature. This means sulfur on the surface of as-synthesized sample is unstable to heat and changed to sulfate when thermal treatment is applied. When thermal treatment is carried out at high temperature, visible light photocatalytic activity is low

because quantity of dopants is not optimized in this research. These results demonstrated that thermal treatment at low temperature exerts a strong influence on the photocatalytic activity of nitrogen and sulfur codoped TiO_2.

5. References

[1] Su-Yeol Ryu, Dong Suk Kim, Jae-Deok Jeon, and Seoung-Yeop Kwak, *J. Phys. Chem. C* **2010**, *114*, 17440-17445

[2] T. Rajh, J. M. Nedeljkovic, L. X. Chen, O. Poluektov, and M. C. Thurnauer, *J. Phys. Chem. B* **1999**, *103*, 3515-3519

[3] Konstantinos C. Christoforidis, Santiago J.A. Figueroa, Marcos Fernandez-Garcia, *Appl. Catal. B Environ.* **2013**, *117*, 310-316

[4] Xiufang Zhang, Yan Gong, Xiaoli Dong, Xinxin Zhang, Chun Ma, Fei Shi, *Mater.Chem. Phys.* **2012**, *136*, 472-476

[5] Xiaobo Chen, Lei Liu, Peter Y. Yu, Samuel S. Mao, *Science* **2011**, *331*, 746-750

[6] L. Gomathi Devi, B. Narasimha Murthy, *Catal. Lett.* **2008**, *125*, 320-330

[7] Jeffrey C.-S. Wu, Chih-Hsien Chen, *J. Photoch. Photobio. C* **2004**, *163*, 509-515

[8] Jiaguo Yu, Quanjun Xiang, Minghua Zhou, *Appl. Catal. B-Environ.* **2009**, *90*, 595-602

[9] Wonyong Choi, Andreas Termin, and Michael R. Hoffmann, *J. Phys. Chem.* **1994**, *98*, 13669-13679

[10] Meng Ni, Michael K. H. Leung, Dennis Y. C. Leung, K. Sumathy, *Renew. Sust. Energ. Rev*. **2007**, *11*, 401-425

[11] Jina Choi, Hyunwoong Park, and Michael R. Hoffmann, *J. Phys. Chem. C* **2010**, *114*, 783-792

[12] Hua Tian, Junfeng Ma, Kang Li, Jinjun Li, *Ceram. Int.* **2009**, *35*, 1289-1292

[13] Maria Vittoria Dozzi, Elena Selli, *J. Photoch. Photobio. C* **2013**, *14*, 13-28

[14] Penghua Wang, Pow-Seng Yap, Teik-Thye Lim, *Appl. Catal. A-Gen.* **2011**, *399*, 252-261

[15] M. Sathish, B. Viswanathan, R. P. Viswanath, Chinnakonda S. Gopinath, *Chem. Mater*. **2005**, *17*, 6349-6353

[16] Stefano Livraghi, Maria Cristina Paganini, Elio Giamello, Annabella Selloni, Cristiana Di Valentin, and Gianfranco Pacchioni, *J. Am Chem. Soc*. **2006**, *128*, 15666-15671

[17] R. Asahi, T. Morikawa, T. Ohwaki, K. Aoki, Y. Taga, *Science* **2001**, *293*, 269-271

[18] Shanmugasundaram Sakthivel, Marcin Janczarek, and Horst Kisch, *J. Phys. Chem. B* **2004**, *108*, 19384-19387

[19] Enrique A. Reyes-Garcia, Yanping Sun, Karla eyes-Gil, and Daniel Raftery, *J. Phys. Chem. C* **2007**, *111*, 2738-2748

[20] Priyanka P. Bidaye, Deepa Khushalani, J. B. Fernandes, *Catal. Lett.* **2010**, *134*, 169-174

[21] Naoto Umezawa, Anderson Janotti, Patrick Rinke, Toyohiro Chikyow, and Chris G. Van de Walle, *Appl. Phys. Lett.* **2008**, *92*, 041104

[22] Hua Tong, Shuxin Ouyang, Yingpu Bi, Naoto Umezawa, Mitsutake Oshikiri, and Jinhua Ye, *Adv. Mater.* **2013**, *24*, 229-251

[23] M. Sathish, R. P. Viswanath, and Chinnakonda S. Gopinath, *J. Nanosci. Nanotechnol.* **2009**, *9*, 423-432

[24] Brundabana Naik, K. M. Parida, and Chinnakonda S. Gopinath, *J. Phys. Chem. C* **2010**, *114*, 19473-19482

[25] Teruhisa Ohno, Miyako Akiyoshi, Tsutomu Umebayashi, Keisuke Asai, Takahiro Mitsui, Michio Matsumura, *Appl. Catal. A-Gen*. **2003**, *265*, 115-121

[26] Changseok Han, Miguel Pelaez, Vlassis Likodimos, Athanassios G. Kontos, Polycarpos Falaras, Kevin O'shea, Dionysios D. Dionysiou, *Apple. Catal. B-Environ.* **2011**, *107*, 77-87

[27] Chanhoi Kim, Moonjung Choi, Jyongsik Jang, *Catal. Commun*. **2010**, *11*, 378-382

[28] XIE, Tonggeng XI, Qinghong ZHANG, and Qingren WU, *J. Mater. Sci. Technol*. **2003**, *19*, 463-466

[29] Yixin Zhao, Xiaofeng Qiu, and Clemens Burda, *Chem. Mater.* **2008**, *20*, 2629-2636

[30] Wingkei Ho, Jimmy C. Yu, Shuncheong Lee, *J. Solid State Chem*. **2006**, *179*, 1171-1176

[31] Dong Suk Kim, Seung-Yeop Kwak, *Appl. Catal. A – Gen*. **2007**, *323*, 110-118

[32] Maria Vittoria Dozzi, Stefano Livraghi, Elio Giamello and Elena Selli, *Photochem. Photobiol. Sci*. **2011**, *10*, 343-349

[33] Cristiana Di Valentin, Gianfranco Pacchioni, Annabella Selloni, Stefano Livraghi, and Elio Giamello, *J. Phys. Chem. B* **2005**, *109*, 11414

[34] Hiroshi Irie, Yuka Watanabe, and Kazuhito Hashimoto, *J. Phys Chem. B* **2003**, *107*, 5483-5486

[35] Taixing Wu, Guangming Liu, and Jincai Zhao, Hisao Hidaka, Nick Serpone, *J. Phys. Chem. B* **1998**, *102*, 5845-5851

[36] Roberta R. Naujok, Robert V. Duevel, and Robert M. Corn, *Langmuir* **1993**, *9*, 1771-1774

[37] Ammar Houas, Hinda Lachheb, Mohamed Ksibi, Elimame Elaloui, Chantal Guillard, Jean-Marie Herrmann, *Appl. Catal. B-Environ.* **2001**, *31*, 145-157

국문초록

본 연구에서는 질소, 황이 코도핑된 TiO_2 가 높은 가시광활성도를 가지는 이유를 규명하기 위해 TiO_2 의 표면과 내부에 존재하는 질소와 황 도펀트 각각의 영향에 대해 연구하였다. 샘플의 결정성과 결정크기, 결정구조를 X 선 회절분석법 (XRD)와 고 배율 투과전자현미경 (HR-TEM) 을 통해 관찰하였다. 광전자 분광기 (XPS)를 통해 도펀트의 함량과 화학적 준위를 관찰한 결과 질소와 황 도펀트는 TiO_2 내부에서 산소 자리를 치환하고 있음을 확인할 수 있었다. NST 샘플의 표면에서 질소는 산소와 결합하여 상대적으로 높은 결합 에너지를 가지고 있었고, 열처리를 진행하지 않은 NST-As 샘플은 기존에 알려진 황 2 가 음이온보다 높은 결합 에너지를 가지고 있었다. TiO_2 내부의 산소를 치환하고 있는 질소와 황 도펀트는 350 도 이상의 온도에서 열처리가 진행됨에 따라서 급격히 외부로 빠져나게 되었다. 열처리가 진행되는 동안 황 도펀트는 표면으로 빠져나가게 되지만, 전체 황 함량은 일정하다는 사실을 유도결합 플라즈마 원자방출분광기 (ICP-AES) 분석을 통해 밝혀내었다. 가시광 영역대의 반사율을 측정하여 밴드갭을 계산한 결과 TiO_2 의 내부와 표면에 존재하는 도펀트가 모두 TiO_2 의 밴드갭을 줄여준다는 사실을 알아내었다.

NST 샘플들의 광활성능을 측정하기 위해 유기염료인 rhodamine B 의 분해거동을 가시광과 자외선을 조사하며 관찰하였다. 분석 결과 TiO_2 의

표면과 내부에 존재하는 도펀트들 모두 재결합 센터로 작용함과 동시에 가시광 활성도를 높여주었다. 가시광을 조사할 때 산소 자리를 치환한 질소 도펀트가 TiO_2 의 밴드갭을 줄여주어 용액상에서의 rhodamine B 분해작용을 촉진시키고 표면에 존재하는 황이 유기 염료들과 상호작용을 통해 디에틸레이션 반응을 촉진시켰다. NST-As 샘플의 경우 상업화된 TiO_2 인 P25 에 비해 7.7 배 빠르게 rhodamine B 를 분해시켰다.

감사의 글

2 년간의 석사과정을 마무리 하면서, 무엇보다도 저를 보살펴주시고 무한한 사랑을 베풀어주신 가족 여러분들께 깊은 감사를 드립니다. 부족한 저를 항상 믿어주시고 응원해주신 덕분에 석사과정을 무사히 마무리할 수 있었습니다.

저의 석사과정을 뒤돌아보면, 성급한 성격 탓에 많은 실수와 시행착오를 겪기도 했고 좌절했던 적도 많았습니다. 하지만 곽승엽 교수님께서 늘 아낌없는 지도와 조언을 통해 저의 연구를 바로잡아주신 덕분에 석사학위논문을 작성할 수 있었습니다. 진심으로 감사 드립니다. 그리고 귀중한 시간을 내어 논문을 심사해주신 장지영 교수님과 안철희 교수님께도 감사 드립니다. 또한 바쁘신 와중에도 저에게 많은 조언을 해주시고 독려해주신 정재우 교수님께도 깊이 감사 드립니다.

비록 짧은 시간이지만 지난 2 년동안 연구실 선배님들께 연구적인 부분뿐만이 아니라 연구실의 구성원으로서의 역할과 책임감에 대해서도 많이 배우게 되었습니다. 늘 인자한 미소와 함께 많은 도움을 주신 성학이형, 제 연구와 실험실 생활에 대해 자신의 일처럼 관심과 열정을 쏟아주신 수열이형, 친근하게 다가와 많은 도움을 주신 형구형, 긍정적이고 활발한 성격으로 저에게 힘을 주신 현중이형, 성실성과 책임감을 가르쳐주신 성용이형, 제가 고민이 있을 때 늘 지혜를 나누어 주신 우혁이형, 실험실 일을 많이 도와주신 효원이형, 그리고 성급한 저에게 여유를 가지게 해주신 지훈이형께 감사의 말씀 드립니다. 그리고 항상 후배들을 배려하고 이해해주는 지환이형, 연구실 일들에 대해 친절하게 가르쳐주신 태선이형, 실험에 대해 많은 조언을 해준 규원이형, 항상 성실한 민영이, 많은 면에서 조언을 해주고 활기찬 기운을 나눠준 승희형, 세심한 배려로 선배들을 기쁘게 해준 예지에게도 깊은 감사 말씀을 전하고자 합니다. 그리고 늘 저에게 많은 힘이 되어준 현지에게 진심으로 감사 드립니다.

지난 2 년간의 경험을 교훈 삼아 앞으로 더욱 보람찬 박사과정을 보낼 수 있도록 노력하겠습니다. 감사합니다.

2014 년 2 월 정준호